



# Exploring the potential of AOX to prevent toxic smoke effects and hypoxia response

Luís Nuno Pereira Esteves  
Dissertação de Mestrado apresentada à  
Faculdade de Ciências da Universidade do Porto  
Biologia Celular e Molecular

2014/2015

MSc

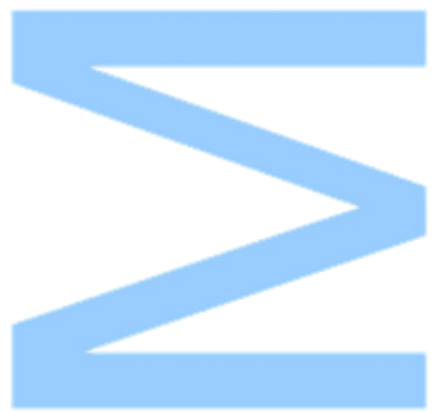
2.º CICLO

FCUP  
UTA  
UH



Exploring the potential of AOX to prevent toxic smoke effects and hypoxia response

Luís Nuno Pereira Esteves



# Exploring the potential of AOX to prevent toxic smoke effects and hypoxia response

Luís Nuno Pereira Esteves

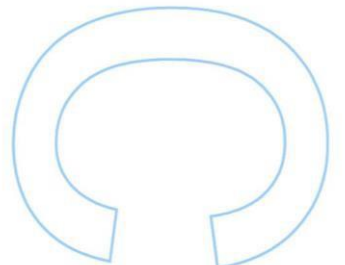
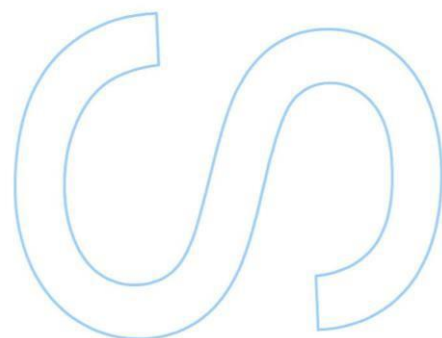
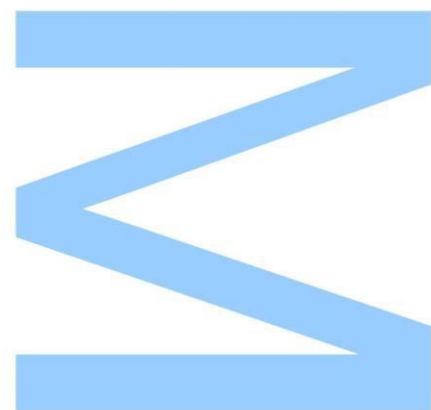
Mestrado em Biologia Celular e Molecular  
Biologia da FCUP  
2014/2015

**Supervisor**

Howard Jacobs, Professor, Universities of Helsinki and Tampere

**Co-Supervisor**

Marten Szibor, MD, Universities of Helsinki and Tampere  
José Pissara, Professor, University of Porto

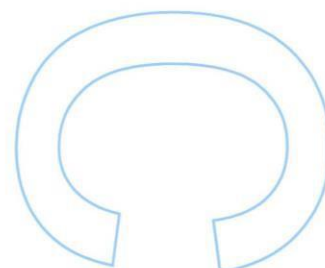
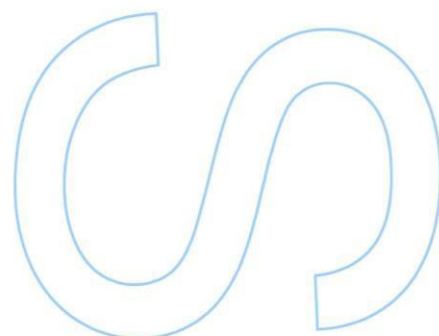
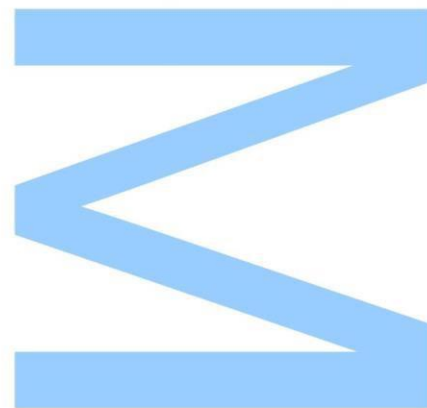




Todas as correções determinadas pelo júri, e só essas, foram efetuadas.

O Presidente do Júri,

Porto, \_\_\_\_ / \_\_\_\_ / \_\_\_\_



# Acknowledgments

Before thanking everyone that contributed to this work, I would quickly thank the institutions that contributed to it. I would like to thank my home University of Porto (UP) and Erasmus programme and Tampere University (UTA) for allowing me and providing financial support to do my dissertation aboard, and lastly I like to thank the Biomedicum and the Viiki Campus of the University of Helsinki (UH) for providing the physical facilities in which this work was performed.

Now moving on to the people, I would like to give a big thanks to my supervisor professor Howy Jacobs for accepting me in his group and for all the help and crucial guidance he provided not only during the dissertation but also prior to my arrival to Finland.

I would like to thank my co-supervisor doctor Marten Szibor for all the guidance and help provided during my time in Howy Lab, which was crucial for the execution of this project. I wish a very successful future for the lab and all its lab members.

I would like to thank my co-supervisor professor José Pissara for accepting me as my local supervisor and also for all the help that both he and professor Susana Pereira provided during my education in the master and in the bachelor's internship.

I would like to give a special thanks to the protein expert Liliya Euro for playing a vital role in the protein part of this work, both in the the executing of the experiments as well as helping to devise solutions to overcome the challenges that arose from the purification process.

I would like to thank everyone in Anu Wartiovaara's Lab, Brendan Battersby's Lab and Henna Tyynismaa's Lab for allowing me to use their facilities and equipment as well for the funny moments during break hours.

I would like to give a big thank you all Howy Lab members for all the support provided in this work, as well as the time spent together talking about science and mostly other topics, a very special thanks to Troy for the friendship and hang outs in Helsinki with the crazy Indian and Antti, and to Maarit for all the patience to have always going to

her to ask technical details, where stuff were and to order things needed to the project, not to mention for the crazy talks during coffee time.

I would like to give a big thanks to both Antti and Praveen which were that always provided crucial help and guidance in the execution of this work, as also a lot of laughs and random out of the blue talks to completely distract me from the stress in the lab, and proved to be great friends to hang out with and watch the crapiest movies with like Meet the Feebles.

I would like to give a very big thanks to all my friends in Portugal, who as always were there when I was out of work and still stressing about things not working or other things, as also to provide support in everything and that are still able to keep up with me despite the long time they have already endured my presence in their life's.

Lastly, both one of the most important, I would like to thank my family for everything they have for me during all my life and for the constant and unconditional support provided.

## Resumo

Doenças mitocondriais, envolvendo disfunções na cadeia cytochromo, estão geralmente associadas com bloqueios a nível do COX, causando disfunções metabólicas e em alguns casos morte.

O uso de tabaco e exposição a fumos tóxicos causam milhões de mortes por ano (segundo a WHO) devido aos seus efeitos adversos em viabilidade celular, e estão associados a muitas doenças respiratórias. Dos 5000 compostos do fumo de cigarros, o cianeto e monóxido de carbono são os mais proeminentes inibidores do COX.

O objetivo primário deste estudo era gerar uma proteína AOX cataliticamente ativa para transfectar células de mamíferos, com potencial farmacológico para compensar deficiências do COX. O objetivo secundário era testar a hipótese de que a expressão de AOX, uma oxidase alternativa ausente nos vertebrados, consegue proteger as células até um certo ponto, do dano causado por fumos tóxicos. Para os objetivos propostos, (1) uma proteína recombinante AOX foi gerada, em sistema de expressão de proteínas recombinantes em procariotas, em conjugação da AOX com um péptido TAT, derivado do vírus de imunodeficiência humana que permite a penetração através de membranas de proteínas a ele conjugadas; e (2) a resposta à exposição a CSE foi analisada e comparada em três linhas celulares diferentes expressando AOX e os seus respetivos controlos WT (293T HEK, MEF e NIH 3T3).

A produção e purificação de uma proteína recombinante membranar é uma tarefa exigente e complexa. Apesar de não ter sido possível obter uma proteína AOX ultra pura, este trabalho forneceu evidências de que a AOX recombinante foi incorporada por células de mamíferos, onde demonstrou atividade catalítica tanto *in vitro* e *ex vivo*. Contrariamente a hipótese inicial, células com expressão de AOX não foram protegidas dos efeitos tóxicos causados por exposição a CSE. Tanto, a proliferação como o número de células viáveis foi reduzido na mesma proporção em células AOX e células controlo.

O objetivo principal de estabelecer um protocolo para produzir e purificar uma AOX cataliticamente ativa foi alcançado com sucesso. Será interessante verificar se a TAT-AOX poderá ser usada para tratamento em modelos *in vitro*, *ex vivo* e eventualmente *in vivo*, de doenças mitocondriais. Quanto ao objetivo secundário, tendo em conta os resultados obtidos neste trabalho não se pode concluir que a AOX confere proteção contra fumos tóxicos, porém é preciso considerar que existem diferenças entre a composição do CSE e dos fumos tóxicos. Portanto, são necessários mais estudos compreensivos usando exposição direta a fumo de cigarro ou métodos de extração de toxinas alternativos. **Palavras-chave:** oxidase alternativa (AOX), extrato de fumo de cigarro (CSE), HIV-derivado transactivador da transcrição, hipoxia, fumo de cigarro.

## Summary

Mitochondrial diseases involving dysfunctions in the cytochrome chain, are generally associated with blockades at level of COX, causing metabolic dysfunctions and in some cases death.

Tobacco use and exposure to toxic smoke causes millions of deaths per year (according to the WHO) due to its adverse effects on cell viability and it is associated with many respiratory diseases. Among the 5000 compounds of the cigarette smoke, cyanide and carbon monoxide are the most prominent inhibitors of COX.

The primary goal of this study was to generate a catalytically active AOX protein to transfect mammalian cells, with the pharmacological potential to compensate for COX deficiencies. The secondary goal was to test the hypothesis that expression of AOX, an alternative oxidase absent in vertebrates, can protect cells to some extent against toxic smoke damage. To achieve the proposed goals, (1) a recombinant AOX protein, in a prokaryotic recombinant protein expression system with AOX being conjugated to a TAT peptide, was generated, TAT is derived from the human immunodeficiency virus and enables cell membrane penetration of the conjugate; and (2) the response of three different AOX-expressing cell lines and their respective WT controls (293T HEK, MEF and NIH 3T3) to CSE was analysed and compared.

Producing and purifying a recombinant membrane protein is complex and challenging. Despite not being able to generate a highly purified AOX protein, this work provided evidence that the recombinant AOX was taken up by mammalian cells, where it was catalytically active *in vitro* and *ex vivo*. Unlike the initial hypothesis, AOX-expressing cells were not protected from toxic effects provoked by exposure to CSE. Both, viable cell number and proliferation were reduced to the same degree in AOX and control cells.

The primary goal to establish a protocol to produce and purify a catalytically active AOX protein was fully reached. It will be interesting to see if TAT-AOX treatment can be used *in vitro*, *ex vivo* and, eventually, *in vivo* in different disease models with mitochondrial impairment. Regarding the secondary goal, from the results obtained in this work it cannot be concluded that AOX confers protection against toxic smoke, however one has to take into account that CSE and CS contents differ. Therefore, more comprehensive studies are needed using direct cigarette smoke exposure or alternative toxin extraction methods.

**Key words:** alternative oxidase (AOX), cigarette smoke extract (CSE), HIV-derived transactivator of transcription, hypoxia, cigarette smoke.

# Index

<b>1- INTRODUCTION</b> .....	<b>1</b>
<b>1.1- Mitochondria: energy and ROS production</b> .....	<b>2</b>
1.1.1- <u>Energy production and substrates</u> .....	2
1.1.2- <u>Respiratory chain and electron flow</u> .....	3
1.1.3- <u>ROS production</u> .....	5
<b>1.2- Tobacco: lethality and hazards to health</b> .....	<b>6</b>
<b>1.3- Alternative oxidase (AOX)</b> .....	<b>7</b>
1.3.1- <u>Function on native systems</u> .....	7
1.3.2- <u>Ciona intestinalis AOX in human health</u> .....	8
<b>1.4- TAT protein</b> .....	<b>9</b>
<b>1.5- Goal</b> .....	<b>10</b>
<b>2- METHODS</b> .....	<b>11</b>
<b>2.1- Production of catalytically active recombinant AOX</b> .....	<b>11</b>
2.1.1- <u>Plasmid engineering</u> .....	11
2.1.2- <u>Bacterial transformation</u> .....	11
2.1.3- <u>Recombinant protein induction</u> .....	12
2.1.4- <u>Protein Purification</u> .....	12
2.1.5- <u>Recombinant AOX activity</u> .....	14
<b>2.2- AOX protection against CSE damage</b> .....	<b>14</b>
2.2.1- <u>Cell lines</u> .....	14
2.2.2- <u>CSE production</u> .....	14
2.2.3- <u>Cell counting and seeding</u> .....	15
2.2.4- <u>Plate-coating</u> .....	15
2.2.5- <u>Growth mediums</u> .....	15
2.2.6- <u>Exposure to CSE</u> .....	16
2.2.7- <u>Evaluation of response mechanisms</u> .....	16
<b>3- RESULTS</b> .....	<b>17</b>
<b>3.1- Purification of catalytically active recombinant AOX</b> .....	<b>17</b>
3.1.1- <u>Recombinant AOX production in bacteria</u> .....	17
3.1.2- <u>Increasing yield of protein in soluble form</u> .....	18
3.1.3- <u>Purification of recombinant AOX</u> .....	21
3.1.4- <u>Recombinant AOX activity</u> .....	23
<b>3.2- AOX protection against CSE damage</b> .....	<b>25</b>
3.2.1- <u>293T HEK cells</u> .....	25
3.2.2- <u>MEFs from Aox-Rosa26</u> .....	27

3.2.3- <u>NIH 3T3 cells</u> .....	31
<b>4- DISCUSSION.....</b>	<b>34</b>
<b>4.1- Recombinant AOX production.....</b>	<b>34</b>
4.1.1- <u>Plasmid engineering</u> .....	34
4.1.2- <u>Protein production</u> .....	35
4.1.3- <u>Protein purification</u> .....	35
4.1.4- <u>TAT AOX activity assay</u> .....	36
<b>4.2- AOX protection against CSE damage .....</b>	<b>38</b>
4.2.1- <u>293T HEK cells</u> .....	38
4.2.2- <u>MEFs from Aox-Rosa26</u> .....	38
4.2.3- <u>NIH 3T3 cells</u> .....	40
<b>4.3- Conclusion .....</b>	<b>41</b>
<b>REFERENCES.....</b>	<b>42</b>

# Figure's list

**FIGURE 1** SCHEMATIC OF THE RESPIRATORY CHAIN. ELECTRON FLOW IS REPRESENTED BY THE RED ARROWS. ....5

**FIGURE 2** GRAPH OF TOBACCO USAGE RISK FACTOR IN 6 OF THE 8 LEADING CAUSES OF DEATH IN THE WORLD. ATTACHED AREAS ARE THE AMOUNT OF DEATH CORRESPONDING TO TOBACCO USAGE IN EACH DISEASE. ADAPTED FROM "WHO REPORT ON THE GLOBAL TOBACCO EPIDEMIC, 2008. ....7

**FIGURE 3** STRUCTURAL 3D MODEL OF CIONA INTESTINALIS AOX (GREEN) SUBUNIT USING TRYPANOSOMAL AOX AS A TEMPLATE FOR HOMOLGY MODELLING (ORANGE) WITH DI-IRON CENTRE, DELETION AND ELONGATION LOOPS ANNOTATED. MODEL DESIGNED BY LILIYA EURO .....9

**FIGURE 4** SCHEME OF PROTEIN PURIFICATION ..... 13

**FIGURE 5** SCHEME OF SUMO CLEAVAGE AND SECOND TAT AOX PURIFICATION ..... 13

**FIGURE 6** SUMO AOX PRODUCTION ANALYSIS: GROWTH MONITORING BY OD<sub>600</sub> MEASUREMENT IN SPECIFIC TIME POINTS (1) AND SDS-PAGE ANALYSIS OF SAMPLES HARVESTED IN SPECIFIC TIME POINTS WITH LOCATION OF SUMO TAT-AOX (APPROXIMATELY 60 KDA) IS HIGHLIGHTED IN RED BOX. (2) ..... 17

**FIGURE 7** SUMO TAT-AOX PRODUCTION ANALYSIS: GROWTH MONITORING BY OD<sub>600</sub> MEASUREMENT IN SPECIFIC TIME POINTS (1) AND SDS-PAGE ANALYSIS OF SAMPLES HARVESTED IN SPECIFIC TIME POINTS WITH LOCATION OF SUMO TAT-AOX (APPROXIMATELY 60 KDA) IS HIGHLIGHTED IN RED BOX. (2). ..... 18

**FIGURE 8** SDS-PAGE OF SUMO TAT-AOX PRODUCTION ANALYSIS OF HOMOGENATE, MEMBRANE FRACTION AND SOLUBLE FRACTION AT DIFFERENT GROWTH TEMPERATURES: ROOM TEMPERATURE (RT), 30 °C AND 37 °C. LOCATION OF SUMO TAT-AOX (APPROXIMATELY 60 KDA) IS HIGHLIGHTED IN RED BOX..... 18

**FIGURE 9** SDS-PAGE OF SUMO TAT-AOX PRODUCTION ANALYSIS OF MEMBRANE FRACTION AND SOLUBLE FRACTION AT GROWN AT 30 °C WITH DIFFERENT IPTG INDUCTION IN LB WITH KANAMYCIN (1) AND LB 1% GLUCOSE WITH KANAMYCIN (2). LOCATION OF SUMO TAT-AOX (APPROXIMATELY 60 KDA) IS HIGHLIGHTED IN RED BOX. .... 19

**FIGURE 10** SDS-PAGE OF SUMO TAT-AOX ANALYSIS OF MEMBRANE FRACTION AND SOLUBLE FRACTION WITH PROTEIN SOLUBILISATION USING DIFFERENT DDM CONCENTRATIONS. LOCATION OF SUMO TAT-AOX (APPROXIMATELY 60 KDA) IS HIGHLIGHTED IN RED BOX..... 20

**FIGURE 11** SDS-PAGE OF SUMO TAT-AOX PRODUCTION ANALYSIS OF HOMOGENATE, MEMBRANE FRACTION AND SOLUBLE FRACTION AT 30 °C AND 37 °C WITH 0,25MM IPTG AND 0,025MM IPTG. LOCATION OF SUMO TAT-AOX SURROUNDED AT RED... 20

**FIGURE 12** SDS-PAGE OF SUMO TAT-AOX PRODUCTION ANALYSIS OF HOMOGENATE, MEMBRANE FRACTION AND SOLUBLE FRACTION GROWN AT 30 °C IN LB KANAMYCIN MEDIUM WITH IRON II SUPPLEMENTATION (1) AND IRON III SUPPLEMENTATION (2). LOCATION OF SUMO TAT-AOX SURROUNDED AT RED. ... 21

**FIGURE 13** WESTERN BLOT OF SUMO-TAT-AOX HIS TRAP AFFINITY CHROMATOGRAPHY PURIFICATION RESULTS. RED RECTANGLES HIGHLIGHT LOCATIONS OF SUMO-TAT-AOX (APPROXIMATE 60 KDA) AND AOX (APPROXIMATE 37 KDA) ..... 21

**FIGURE 14** WESTERN BLOT OF SUMO-TAT-AOX DESALTING AND SUMO CLEAVAGE (CLEAVED) RESULTS. RED RECTANGLES HIGHLIGHT LOCATIONS OF SUMO-TAT-AOX (APPROXIMATE 60 KDA) AND AOX (APPROXIMATE 37 KDA) ..... 22

**FIGURE 15** WESTERN BLOT OF SUMO-TAT-AOX PURIFICATION PROTOCOL RESULTS, USING IMIDAZOLE IN THE DESALTING STEP (BEFORE CLEAVAGE) AND

ATTEMPTING TO PURIFY TAT-AOX FROM THE OTHER PROTEINS IN THE CLEAVAGE PRODUCT. RED RECTANGLES HIGHLIGHT LOCATIONS OF SUMO-TAT-AOX (APPROXIMATE 60 KDA), TAT-AOX (APPROXIMATE 40 KDA) AND AOX (APPROXIMATE 37 KDA).....22

**FIGURE 16** *IN VITRO* TAT-AOX ACTIVITY RESULTS OF AMA INCUBATION IN NIH 3T3 CELL LINES: *WILD TYPE* (WT), AOX AND *WILD TYPE* WITH TAT-AOX DILUTED IN GROWTH MEDIUM (WT+TAT-AOX). DEAD CELLS APPEAR AS ROUND AND BRIGHT CELLS. ....23

**FIGURE 17** RESULTS OF NIH 3T3 WT AND EXPOSED TO ENRICHED TAT-AOX (TAT), INCUBATED IN DMEM WITH 100 µM AMA FOR 48 H, IN BOTH NUMBER OF THOUSANDS OF VIABLE CELLS (ON THE LEFT) AND RATIO BETWEEN LIVE CELLS IN TESTED CONDITION AND CONTROL CONDITION WITH NO AMA (ON THE RIGHT). SIGNIFICANCE OF THE DIFFERENCE IN THE MEASURED VALUES IS REPRESENTED BY THE STARS (\*), THE MORE STARS REPRESENTED THE HIGHER THE SIGNIFICANCE .....24

**FIGURE 18** *EX VIVO* TAT-AOX ACTIVITY RESULTS OF PERFUSION OF A WT LUNG WITH TAT-AOX (POINT OF PERFUSION INDICATED BY ARROW) IN PHYSIOLOGICAL BUFFER. THIS FIGURE IS SHOWN WITH THE PERMISSION OF NATASCHA SOMMER. ....25

**FIGURE 19** RESULTS OF HEK CELLS INCUBATED IN CSE DILUTIONS IN DMEM LOW GLUCOSE FOR 24 H IN BOTH NUMBER OF THOUSANDS OF VIABLE CELLS (ON THE LEFT) AND RATIO BETWEEN LIVE CELLS IN TESTED CONDITION AND CONTROL CONDITION WITH 0% CSE (ON THE RIGHT). ....26

**FIGURE 20** RESULTS OF HEK CELLS INCUBATED IN CSE DILUTIONS IN DMEM GALACTOSE FOR 24 H IN BOTH NUMBER OF THOUSANDS OF VIABLE CELLS (ON THE LEFT) AND RATIO BETWEEN LIVE CELLS IN TESTED CONDITION AND CONTROL CONDITION WITH 0% CSE (ON THE RIGHT).....27

**FIGURE 21** RESULTS OF MEF CELLS INCUBATED IN CSE DILUTIONS IN DMEM HIGH GLUCOSE FOR 48 H IN BOTH NUMBER OF THOUSANDS OF VIABLE CELLS (ON THE LEFT) AND RATIO BETWEEN LIVE CELLS IN TESTED CONDITION AND CONTROL CONDITION WITH 0% CSE (ON THE RIGHT). ....28

**FIGURE 22** RESULTS OF MEF CELLS INCUBATED IN CSE DILUTIONS IN DMEM GALACTOSE FOR 48 H IN BOTH NUMBER OF THOUSANDS OF VIABLE CELLS (ON THE LEFT) AND RATIO BETWEEN LIVE CELLS IN TESTED CONDITION AND CONTROL CONDITION WITH 0% CSE (ON THE RIGHT).....28

**FIGURE 23** RESULTS OF MEF CELLS INCUBATED IN CSE DILUTIONS IN DMEM LOW GLUCOSE (5%FBS) FOR 24 H IN BOTH NUMBER OF THOUSANDS OF VIABLE CELLS (ON THE LEFT) AND RATIO BETWEEN LIVE CELLS IN TESTED CONDITION AND CONTROL CONDITION WITH 0% CSE (ON THE RIGHT).....29

**FIGURE 24** RESULTS OF MEF CELLS INCUBATED IN CSE DILUTIONS IN DMEM GALACTOSE (5%FBS) FOR 24 H IN BOTH NUMBER OF THOUSANDS OF VIABLE CELLS (ON THE LEFT) AND RATIO BETWEEN LIVE CELLS IN TESTED CONDITION AND CONTROL CONDITION WITH 0% CSE (ON THE RIGHT). ....30

**FIGURE 25** RESULTS OF MEF CELLS INCUBATED IN CSE DILUTIONS IN DMEM GALACTOSE (5%FBS) FOR 48 H IN BOTH NUMBER OF THOUSANDS OF VIABLE CELLS (ON THE LEFT) AND RATIO BETWEEN LIVE CELLS IN TESTED CONDITION AND CONTROL CONDITION WITH 0% CSE (ON THE RIGHT). ....30

**FIGURE 26** RESULTS OF MEF CELLS INCUBATED IN CSE DILUTIONS IN DMEM GALACTOSE (5%FBS) FOR 48 H, WITH PREVIOUS 24 H INCUBATION IN THE SAME MEDIUM WITH 2% FBS, IN BOTH NUMBER OF THOUSANDS OF VIABLE CELLS (ON THE LEFT) AND RATIO BETWEEN LIVE CELLS IN TESTED CONDITION AND CONTROL CONDITION WITH 0% CSE (ON THE RIGHT).....31

**FIGURE 27** RESULTS OF NIH 3T3 CELLS INCUBATED IN CSE DILUTIONS IN DMEM LOW GLUCOSE FOR 24 H, IN BOTH NUMBER OF THOUSANDS OF VIABLE CELLS (ON THE LEFT) AND RATIO BETWEEN LIVE CELLS IN TESTED CONDITION AND CONTROL CONDITION WITH 0% CSE (ON THE RIGHT)..... 32

**FIGURE 28** RESULTS OF MEF CELLS INCUBATED IN CSE DILUTIONS IN DMEM GALACTOSE FOR 24 H, IN BOTH NUMBER OF THOUSANDS OF VIABLE CELLS (ON THE LEFT) AND RATIO BETWEEN LIVE CELLS IN TESTED CONDITION AND CONTROL CONDITION WITH 0% CSE (ON THE RIGHT)..... 32

**FIGURE 29** RESULTS OF MEF CELLS INCUBATED IN CSE DILUTIONS IN DMEM GALACTOSE FOR 48 H, IN BOTH NUMBER OF THOUSANDS OF VIABLE CELLS (ON THE LEFT) AND RATIO BETWEEN LIVE CELLS IN TESTED CONDITION AND CONTROL CONDITION WITH 0% CSE (ON THE RIGHT)..... 33

**FIGURE 30** RESULTS OF MEF CELLS INCUBATED IN CSE DILUTIONS IN DMEM GALACTOSE FOR 48 H, WITH PREVIOUS 24 H INCUBATION IN THE SAME MEDIUM WITH 2% FBS, IN BOTH NUMBER OF THOUSANDS OF VIABLE CELLS (ON THE LEFT) AND RATIO BETWEEN LIVE CELLS IN TESTED CONDITION AND CONTROL CONDITION WITH 0% CSE (ON THE RIGHT). ..... 33

## Table's List

**TABLE 1** DETAILS OF MEDIUM SUPPLEMENTS AND SERUM CONCENTRATION FOR EACH CELL TYPE USED. .... 16

## Abbreviations' list

FULL NAME	ABBREVIATION
ADENOSINE-DI-PHOSPHATE	ADP
ANTIMYCIN A	AMA
ADENOSINE-TRI-PHOSPHATE	ATP
ALTERNATIVE OXIDASE	AOX
CALF BOVINE SERUM	CBS
CHRONIC OBSTRUCTIVE PULMONARY DISEASE	COPD
CIGARETTE SMOKE	CS
CIGARETTE SMOKE CONDENSATE	CSC
CIGARETTE SMOKE EXTRACT	CSE
CYTOCHROME C	Cyt c
CYTOCHROME C OXIDASE	COX
DEOXYRIBONUCLEIC ACID	DNA
DIMETHYL SULFOXIDE	DMSO
DODECYLMALTOSE	DDM
DULBECCO'S MODIFIED EAGLE'S <i>MEDIUM</i>	DMEM
DULBECCO'S PHOSPHATE BUFFERED SALINE	DPBS
ELECTRON TRANSFER CHAIN	ETC
ESCHERICHIA COLI	E. coli
FETAL BOVINE SERUM	FBS
FLAVIN ADENOSINE DINUCLEOTIDE	FADH <sub>2</sub>
FLOW THROUGH	FT
GREEN FLUORESCENT PROTEIN	GFP
HIV-DERIVED TRANSACTIVATOR OF TRANSCRIPTION	TAT
HYDROGEN PEROXIDE	H <sub>2</sub> O <sub>2</sub>
HYDROXYL ANION	OH•
HYPOXIA	HOX
INTERMEMBRANE SPACE	IS
ISOPROPYL-BETA-D-THIOGALACTOPYRANOSIDE	IPTG
LURIA-BROTH	LB
MESSENGER RIBONUCLEIC ACID	mRNA
MOUSE EMBRYONIC FIBROBLAST CELLS	MEFs
NICOTINAMIDE ADENOSINE DINUCLEOTIDE	NADH
PERFUSED WEIGHTED	PW
PHOSPHATE BUFFERED SALINE	PBS
PROTEIN TRANSDUCTION DOMAIN	PTD
PULMONARY ARTERIAL PRESSURE	PAP
ROOM TEMPERATURE	RT
OXIDATIVE PHOSPHORYLATION	OXPHOS
RESPIRATORY CHAIN	RC
SUPEROXIDE	O <sub>2</sub>
TRICARBOXYLIC ACID	TCA
UBIQUINOL	QH <sub>2</sub>
WILD TYPE	WT
WORLD HEALTH ORGANIZATION	WHO

# 1- Introduction

Many species, but not mammals, harbour enzymes with the ability to branch the classical respiratory chain, e.g. alternative oxidase (AOX), which is a non-proton motive, inner mitochondrial membrane protein. AOX transfers electrons directly from ubiquinol ( $\text{QH}_2$ ) to oxygen thereby preventing reactive oxygen species (ROS) overproduction when complexes III or IV of the respiratory chain are blocked<sup>(1, 2)</sup>. Due to its low affinity to  $\text{QH}_2$ , as compared to complex III, AOX is catalytically active only under conditions when the cytochrome part of the respiratory chain (complex III and IV) is disabled, thus not interfering with the mitochondrial adenosine-tri-phosphate (ATP) production under unstressed conditions<sup>(2)</sup>.

Due to its characteristics, *Ciona intestinalis* AOX has been used as a tool to compensate mitochondrial dysfunctions related to the respiratory chain and study disease etiologies. The results obtained so far give evidence that AOX can compensate for cytochrome c oxidase (COX) deficiencies in mammalian cells *in vitro*<sup>(3, 4)</sup> and flies *in vivo*. Furthermore, it is clear that a lack of ATP production is only one reason for cellular dysfunction. As important seems to be the ability of AOX to minimize oxidative damage by stopping the excess production of mitochondrial ROS<sup>(5, 6)</sup>, to keep the tricarboxylic acid (TCA) cycle functional as well as conferring resistance to respiratory inhibitors<sup>(7)</sup>.

Toxic smoke and exposure to cigarette smoke (CS), is one of the biggest threats to public health. According to the World Health Organization (WHO), 6 million deaths per year worldwide are attributed to smoking<sup>(8)</sup>. It is widely accepted that smoking can cause chronic lung diseases such as cancer, emphysema, and chronic obstructive pulmonary disease (COPD) among others<sup>(9, 10)</sup>. Many of these diseases are associated with inflammation and oxidative stress in the pulmonary tissue.

From the more than 5000 components present in the CS, many have already been identified as carcinogenic and hazardous<sup>(11)</sup>. The oxidative stress caused by smoke in the lung tissues, is mainly associated with the ability of some smoke compounds to interact with and inhibit the mitochondrial respiratory chain (RC) complexes<sup>(12)</sup> and a decrease in the concentration of anti-oxidant enzymes<sup>(13)</sup>. These conditions lead to an increase in the production of reactive oxygen species (ROS)<sup>(14)</sup> and its accumulation inside the cells as well as hydrolysis of ATP in order to maintain the mitochondrial membrane potential. The most potent inhibitors of the respiratory chain in CS are cyanide<sup>(11)</sup> and carbon monoxide<sup>(15, 16)</sup>, both inhibit COX.

In this work it was speculated that AOX could be used as a therapeutic to reduce or prevent damage caused by toxic smoke exposure. This hypothesis has been thoroughly tested *in vitro* by exposing different mammalian cell lines to cigarette smoke extract (CSE). More importantly, we aimed at the purification of a recombinant, catalytically active AOX protein.

In the following section a bibliographic survey will be presented, regarding mitochondrial energy and ROS production, the hazards of CS, as well as an overview on AOX in general and a brief state of the HIV-derived transactivator of transcription (TAT) protein.

## 1.1- Mitochondria: energy and ROS production

Mitochondria are one of the most metabolic active organelles in the cell; one major role is to synthesize ATP by oxidative phosphorylation. However they also are thermogenic, which is due to the energy dissipation in the form of heat during the ATP production, e.g. under low temperature conditions mitochondria can favour energy dissipation, thereby increasing heat production<sup>(17)</sup>. Furthermore, mitochondria harbour important metabolic circuits and regulate cellular ion homeostasis, e.g. by buffering  $\text{Ca}^{2+}$  to control its available in the cytoplasm<sup>(18)</sup>. Recently, several articles have been published highlighting the role of mitochondria in cell signalling<sup>(19-21)</sup>. Mitochondria are shown to initiate different pathways such as the programmed cell death (apoptosis), an important process to eliminate damaged or infected cells, with cytosolic  $\text{Ca}^{2+}$  being the signal for mitochondrial membrane permeabilisation and release of pro-apoptotic proteins<sup>(19, 20)</sup>; or autophagy, a process that involves the digestion and recycling of biomolecules to prevent cellular dysfunctions. Mitochondria provide membranes for the formation of autophagosomes thereby also regulating mitophagy to turnover dysfunctional organelles, e.g. those damaged by ROS<sup>(19, 22)</sup>.

### 1.1.1- Energy production and substrates

Production of ATP is one of the most important metabolic processes in a cell. Without ATP, cells would not be viable and would eventually die. ATP is the universal energy carrier produced by the breakdown of covalent ligations between molecules; the energy released from the break of the ligation is used to phosphorylate adenosine-diphosphate (ADP) giving rise to ATP<sup>(23)</sup>. In mammalian cells two major processes produce ATP: (1) glycolysis in the cytosol of the cell and (2) oxidative phosphorylation (OXPHOS) in the mitochondrial matrix (aerobic respiration).

Glycolysis is the process of oxidizing sugar molecules to produce ATP. In this process a six carbon molecule (glucose) is broken down to two tri-carbon molecules (pyruvate), with a net yield of two ATP molecules and two molecules of nicotinamide adenosine dinucleotide (NADH)<sup>(23)</sup>.

In normoxia, the pyruvate will be used for aerobic respiration. In this process the pyruvate will be imported to the mitochondrial matrix where it enters the TCA cycle. A series of conversions and oxidative reactions produces high-energy electrons that will be carried as NADH and flavin adenosine dinucleotide (FADH<sub>2</sub>) to the inner membrane's respiratory chain (RC). In the RC the electrons will be transported along the protein complexes, through oxidative reactions with oxygen being the final electron acceptor. To create an electrochemical gradient the flow of electrons is coupled with the pumping of protons from the mitochondrial matrix to the intermembrane space (IS) (mitochondrial membrane potential). Thus mitochondrial respiration generates a proton driven potential that is used by the F1F0 ATP synthase to phosphorylate ADP to generate ATP<sup>(24)</sup>.

It has been shown that under different culture conditions cells can adapt their metabolism and ATP production. This phenomenon can be facilitated to study mitochondrial functions, e.g. when grown in high concentrations of glucose, cells favour glycolysis over OXPHOS causing a decrease in the mitochondrial activity<sup>(25)</sup>. Contrary, under glucose starvation or replacement with glutamine or galactose, cells rely more on oxidative phosphorylation for ATP production<sup>(25-27)</sup>. Galactose is a glucose isomer that needs to be converted to glucose before it can be used as a substrate, this conversion consumes ATP and therefore yields no ATP production by glycolysis forcing the cells to compensate by increasing the yield of the OXPHOS pathway<sup>(25)</sup>. In contrast, glutamine is used directly in the TCA cycle as an alternative substrate to pyruvate<sup>(26)</sup>, bypassing the glycolysis pathway.

### **1.1.2- Respiratory chain and electron flow**

The electron transfer chain (ETC) is located in the inner mitochondrial membrane and is the major part of the RC. Its role is to transfer electrons from substrates originated in the TCA (NADH, FADH<sub>2</sub>) to oxygen. The ETC consists of four complexes in which three (complexes I, III, IV) are proton pumps. Complex II is an electron entry point. All complexes are integral membrane proteins that contain metal ions at their centre, such as iron or copper, and the oxidative potential of the complexes is such that a unidirectional flow of electrons along the chain is ensured among the complexes<sup>(24)</sup>.

The first complex is the NADH dehydrogenase (complex I). This complex accepts electrons from NADH and transfers them to the ubiquinone, with the pumping of four protons to the intermembrane space (IS) of the mitochondria<sup>(28)</sup>.

The succinate:ubiquinone oxidoreductase (complex II) is the only respiratory complex that is not proton pumping. It accepts electrons from the  $\text{FADH}_2$ , originating from succinate oxidation and also transfers the electrons to ubiquinone<sup>(28)</sup>.

Ubiquinone function in the RC is to accept electrons (becoming  $\text{QH}_2$ ) from the complexes I and II and transfer them to the Q-cytochrome *c* oxidoreductase (complex III)<sup>(28)</sup>. Complex III is a less effective proton pump than complex I. It pumps two protons to the IS upon receiving and transferring the electrons from  $\text{QH}_2$  to oxidized cytochrome *c* (Cyt *c*)<sup>(28)</sup>. However, as complex III can only transfer one electron at a time to Cyt *c*, an intermediary process, named Q-cycle<sup>(29)</sup> is needed. In this cycle, both a  $\text{QH}_2$  molecule and a ubiquinone molecule will bind to different sites of complex III. The  $\text{QH}_2$  molecule bound to the complex III Q-site will transfer one of its electrons to Cyt *c*, with the pumping of two protons to the IS associated with this step. The other electron will be transferred to the bound ubiquinone, giving rise to a semiquinone, giving the instability of the semiquinone another  $\text{QH}_2$  is needed to complete the cycle. Therefore the former  $\text{QH}_2$  will return to the Q-pool as a ubiquinone, while another  $\text{QH}_2$  molecule will bind to the Q-site and transfer one of its electrons to Cyt *c* and the other to the semiquinone, giving rise to an oxidized ubiquinone. This oxidized ubiquinone will bind to two protons from the mitochondrial matrix becoming  $\text{QH}_2$  and re-entering the Q-cycle.

Cyt *c* transfers its electrons to COX (complex IV), which is also a proton pump, and transfers the received electrons to the molecular oxygen. The reduced oxygen will interact with two free protons in the matrix giving rise to one water molecule and finalizing the electron transfer<sup>(28)</sup>.

The last complex in the RC is the ATP synthase (complex V). This complex uses the proton driven force generated by ETC to synthesize ATP, by enabling the influx of protons from the IS to the matrix<sup>(28)</sup>. Under low  $\text{O}_2$  levels (ischemia/hypoxia) conditions the ATP synthase can be partially reversed leading to a hydrolysis of ATP coupled to outward pumping of protons in order to retain the mitochondrial membrane potential<sup>(30)</sup>, and to avoid excess ROS production<sup>(30)</sup>.

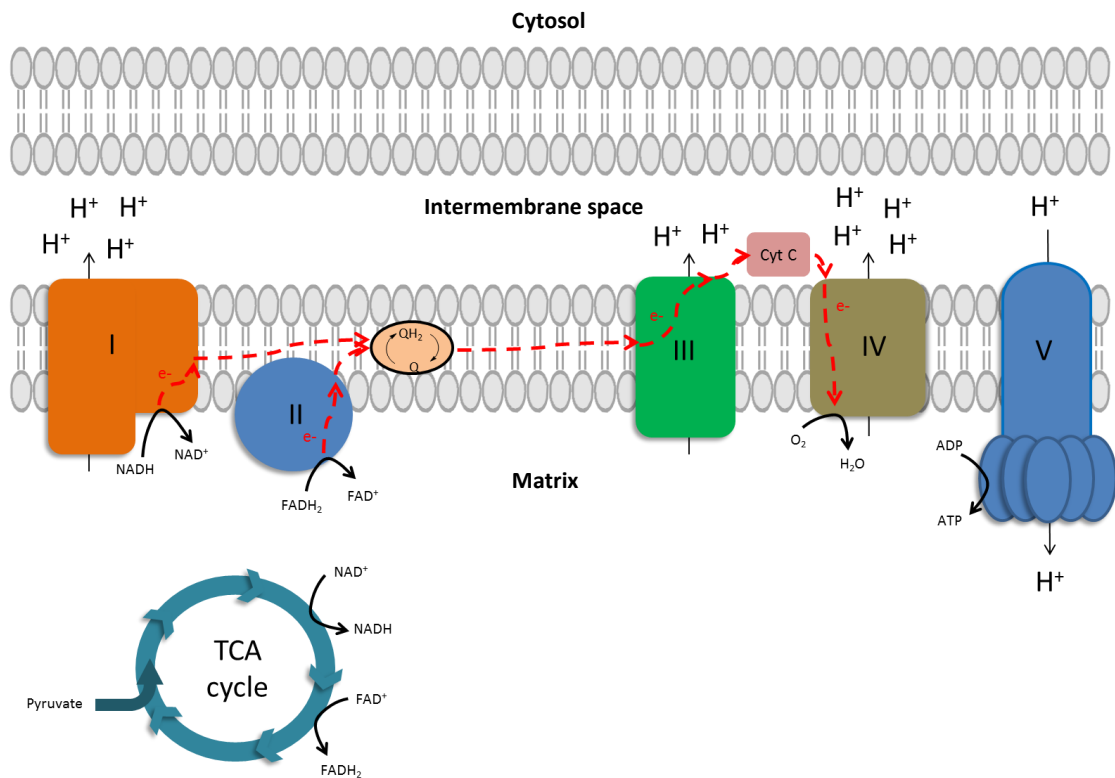


**Figure 1** Schematic of the respiratory chain. Electron flow is represented by the red arrows.

### 1.1.3- ROS production

The term ROS is used to describe a group of O<sub>2</sub> derived radicals (O<sub>2</sub><sup>-</sup>, H<sub>2</sub>O<sub>2</sub> and OH•) that are able to interact with and damage the cell biomolecules. Superoxide (O<sub>2</sub><sup>-</sup>) is the precursor of the hydrogen peroxide (H<sub>2</sub>O<sub>2</sub>) and hydroxyl anion (OH•), and the major organelle involved in its production in mammalian cells is the mitochondrion.

Under normal conditions small amounts of ROS are produced by electrons leaking from the ETC to O<sub>2</sub>, however no damage is done to the cell due to the presence of anti-oxidant enzymes<sup>(31)</sup>. Oxidative damage occurs when the ROS production is greater than the amount of ROS that the anti-oxidant enzymes can neutralize.

Inside the mitochondria eight factors have been identified that contribute to ROS production<sup>(32)</sup>, however only complex I and III are considered to be major ROS producers.

Complex I can produce ROS by direct and indirect electron flow, in both cases the ratio of NADH/NAD<sup>+</sup> and the reduce state of the Q-pool plays a crucial role in the amount of ROS produced. Under direct electron flow when the RC is reduced, and therefore the Q-pool becomes highly reduced, the electrons coming from the NADH will not be transferred to ubiquinone and will leak to the O<sub>2</sub> in the matrix creating O<sub>2</sub><sup>-</sup><sup>(33)</sup>. This

situation can be caused by mutations, dysfunctions or inhibitors of the RC which disables the electron transfer from complex IV to O<sub>2</sub> increasing the reduction state of the Q-pool<sup>(14)</sup>. Complex I is rotenone sensitive and in the presence of this inhibitor the electrons from NADPH will be leaked from complex I to O<sub>2</sub> generating excess amounts of ROS. When complexes III or IV are inhibited, electrons can flow from complex II to complex I, a phenomenon called reverse electron flow. This causes a leak of electrons from complex I directly to O<sub>2</sub> as well as an increase in the NADH/NAD<sup>+</sup> ratio, which favours ROS production in the IS<sup>(14)</sup>.

Complex III produces large amounts of ROS in the presence of its inhibitor antimycin A (AMA). This causes a transfer of electrons from the Q-cycle to O<sub>2</sub>, generating ROS in both the mitochondrial matrix and IS. In the absence of inhibitors, the ROS production by complex III is minimal when compared to the amounts produced by complex I<sup>(14)</sup>.

## 1.2- Tobacco: lethality and hazards to health

Tobacco is a legal drugs that kills people when used according to its purpose. Around the globe smoking kills more than five million people by direct smoking and six hundred thousand by second hand smoking, per year and if the smoking trend does not change, around eight million people per year around the globe are estimated to die by 2025. Furthermore, the deaths annually attributed to smoking are superior to the combined deaths per year of tuberculosis, HIV/AIDS and malaria<sup>(34)</sup>. The use of tobacco is a risk factor in 6 of the 8 leading diseases in the world, significantly contributing to respiratory diseases such as COPD and cancer in the respiratory tracks (Figure 2).

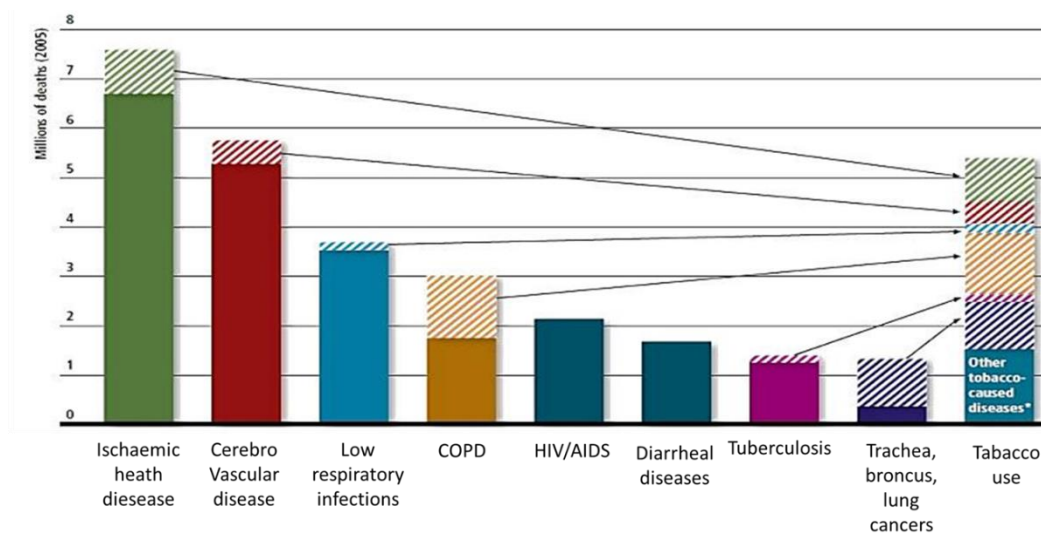


**Figure 2** Graph of tobacco usage risk factor in 6 of the 8 leading causes of death in the world. Attached areas are the amount of death corresponding to tobacco usage in each disease. Adapted from “WHO Report on the global tobacco epidemic, 2008.

Many of the CS components are hazardous to health, Talhout and co-workers published a list of 98 hazards components in CS with their respective endpoints<sup>(11)</sup>. Although the mechanism and pathways by which CS harms the cell are not yet fully understood, the impact of smoking on health is very well established. Knowing that CS contains cyanide, and to a lesser degree carbon monoxide, an inhibition of complex IV is likely, leading to mitochondrial damage.

It is known that CS damage is in part mediated by mitochondria as shown by Li et al. (2014) work, which shown that it was possible to attenuate CS damage by transferring mitochondria from stem cells epithelial airway cells<sup>(35)</sup>.

CS causes inflammation and increases oxidative stress, both in *in vivo* and *in vitro* models<sup>(9)</sup>. Even short term CS exposure is enough to cause significant changes in in alveolar cells metabolism<sup>(12)</sup>. Furthermore, CS inhibits complexes of the RC, thereby decreasing the levels of ATP and increasing the intracellular ROS concentration, causing mitochondrial fission impairment<sup>(13)</sup> and a metabolic shift from apoptosis to necrosis in lung cells<sup>(36)</sup>.

### 1.3- Alternative oxidase (AOX)

Mitochondrial dysfunctions and especially blockades in the RC are almost always lethal. To cope with such dysfunctions some organisms have developed mechanisms or alternative pathways which are able to overcome these metabolic dysfunctions and limit ROS overproduction in the mitochondria. One such way is to bypass the blocked complex of the RC preventing the back-flow of electrons that would escape and generate ROS.

Such a bypass system has evolved in plants, many microorganisms and metazoan. They counteract RC inhibition, especially complex III and IV, with the presence of a cyanide resistant AOX<sup>(37)</sup>, in their RC. AOX is a mitochondrial inner membrane protein that transfers electrons from QH<sub>2</sub> directly to O<sub>2</sub>, thus enabling a bypass of the cytochrome part of the RC<sup>(38)</sup> allowing the organism expressing it to cope with mitochondrial blockades in the cytochrome chain.

#### 1.3.1- Function on native systems

In plants a natural and unavoidable mitochondrial blockade happens daily caused by the presence of sunlight. During photosynthesis the majority of ADP is directed to chloroplast and the intracellular ATP levels increase, in such conditions, the

mitochondrial membrane potential decreases and oxidation of substrate is almost stopped, therefore any electrons entering the RC would easily be leaked and generate ROS<sup>(39)</sup>.

AOX plays an important role in keeping the mitochondrial metabolism active<sup>(40)</sup>, which is essential to plants as some metabolic reactions only happen in the mitochondria. Since it enables the transfer of electrons from the reduced Q-pool of the RC to O<sub>2</sub> it assures the maintenance of a membrane potential as well as the availability of NAD<sup>+</sup> to other metabolic cycles, e.g. the TCA cycle. AOX has a very low affinity to QH<sub>2</sub> compared to complex III, therefore it cannot overtake the bypass mechanism under normal conditions. Thus, AOX is functionally active only when the Q-pool is highly reduced<sup>(41, 42)</sup>.

### **1.3.2- *Ciona intestinalis* AOX in human health**

With the current advance in molecular biology it is easy to integrate a foreign gene into the mammalian genome. AOX has a wide expression in the lower organism, plants and some animal phyla<sup>(37)</sup>, however for some reason it is absent in the mammals. Nonetheless, its expression in some animal phyla provides a pathway of expressing AOX in human cells, since the phylogenetic proximity of the phyla increase the chance of successfully expressing a catalytically active AOX in a heterologous system. Therefore, taking into account that AOX could be a potential cure for some mitochondrial diseases in mammals, provided all the reasons to engineer AOX mammalian cells.

*Ciona intestinalis* is the closest species to chordates harbouring AOX protein. In terms of structure it resembles AOX proteins in other species, possessing a di-iron centre, however in comparison to the widely used *Trypanosoma* AOX it possesses two highly positive charged loops (Figure 3). *Ciona intestinalis* AOX, was successfully used by Hakkaart et al. (2006) to produce stable AOX human cell lines resistant to cyanide<sup>(7)</sup>. This pioneering work opened the path for testing the possibility of AOX to rescue mitochondrial dysfunctions. Furthermore, AOX can be a possible treatment for mitochondrial diseases, since a wide spectrum of diseases ranging from encephalomyopathy and cardiomyopathy in early childhood to neurodegenerative disease in the elderly are associated with complex IV deficiencies<sup>(39)</sup> and there are currently no known treatments available.

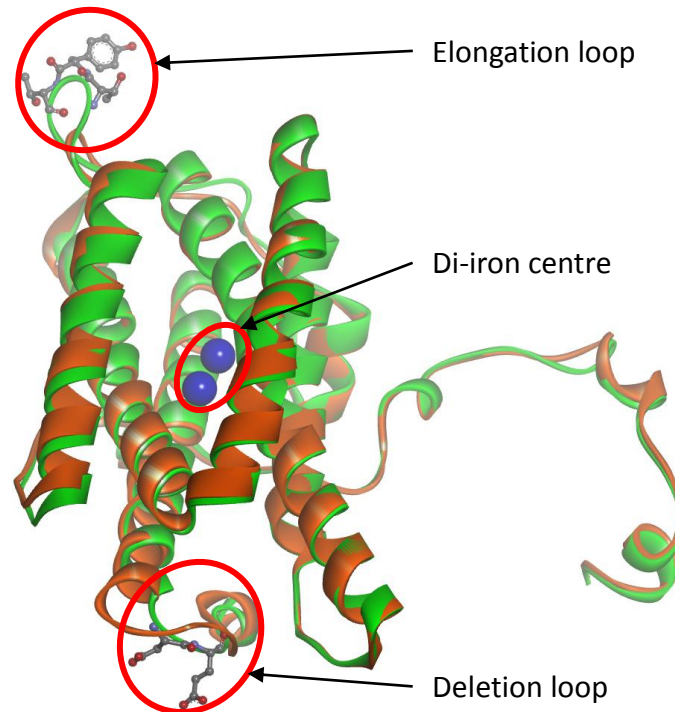


**Figure 3** Structural 3D model of *Ciona intestinalis* AOX (green) subunit using *Trypanosoma* AOX as a template for homology modelling (orange) with di-iron centre, deletion and elongation loops annotated. Model designed by Liliya Euro

## 1.4- TAT protein

An effective protein delivery to and correct intracellular targeting in eukaryotic cells has great impact on medical treatments and molecular studies. The discovery that HIV-1 TAT protein could cross almost every eukaryotic cell membrane, including the nuclear membrane, when added to the culture medium<sup>(43, 44)</sup> was the first step to test if fusion of TAT to a recombinant proteins would allow its efficient transfection. Further studies showed the existence of a protein transduction domain (PTD) in the TAT protein was responsible for the ability of crossing the cellular membranes by a not yet understood mechanism which is independent of receptor, transporter or endocytosis<sup>(45, 46)</sup>. These findings supported the development of applications of an intracellular delivery system<sup>(47)</sup>, which have been used in molecular studies, in particular to deliver an alternative respiratory chain enzyme Ndi1<sup>(48)</sup> *in vivo* to rat heart after ischemia-reperfusion<sup>(49, 50)</sup>.

## 1.5- Goal

The goal of this work was to generate a recombinant AOX protein purified in heterologous systems that can be used as a transfectant to rescue mammalian cells exposed to toxins. Furthermore, it was also aimed to test if AOX could be used as a therapeutic to reduce or prevent cellular damage caused by exposure to CSE as a makeshift of cigarette smoke. We tested the susceptibility of cells expressing AOX to CSE in varying growth mediums. Therefore, the work was structured into two separate projects:

1. To test the production and purification of a catalytically active AOX in heterologous systems, and its delivery to mammalian cells.
2. To test that AOX expression is able to confer some degree of protection to CSE damage in mammalian cells.

## 2- Methods

In order to achieve the goals of this project, both the concepts were tested separately.

1. Production of AOX protein in heterologous expression systems, *Escherichia coli* BL21 (DE3) and *Rosetta 2*, followed by purification using affinity chromatography.
2. Analysing the effect of CSE to induce physiological response in cell lines with and without AOX expression.

### 2.1- Production of catalytically active recombinant AOX

#### 2.1.1- Plasmid engineering

Plasmids for the generation of recombinant AOX were designed as follows: a SUMO<sup>(51)</sup> protein sequence was fused upstream to the *Ciona intestinalis* AOX sequence (SUMO-AOX) with the pET30<sup>(52)</sup> vector (containing a HIS tag) as backbone (Champion pET Sumo expression, Thermo Fisher). Control plasmid was generated with a catalytically inactive (due a single a point mutation) AOX sequence. A second set of plasmids was engineered in the same way, which had an additional TAT<sup>(47)</sup> protein upstream of the AOX sequence and downstream of the SUMO protein sequence (SUMO-TAT-AOX). Restriction enzyme digest and Sanger sequencing were used to validate all the generated plasmids.

#### 2.1.2- Bacterial transformation

Bacterial strains optimized for recombinant protein expression, such as *Escherichia coli* BL21 (DE3) one shot cells (Life Technologies) and *Rosetta 2* were transformed using the engineered plasmids.

One vial of *E. coli* BL21 (DE3) was thawed on ice, followed by addition of 5 ng of plasmid deoxyribonucleic acid (DNA) and incubated on ice for 30 min. Sample were heated to 42 °C for 30 s (heat shock) and immediately transferred to ice followed by addition of 250 mL Luria-Broth (LB) growth medium and incubation at 37 °C with 200 rpm shaking for 1 h. Sample was transferred to 10 mL LB medium (Life Technologies) with kanamycin (50 µg/mL) and incubated overnight 37 °C with 200 rpm .

One vial of chemically competent *E. coli* *Rosetta 2* were thawed on ice and ice cold transformation reaction composed of 10 µl 5x KCM (500 mM KCl, 150 mM CaCl<sub>2</sub> and 250 mM MgCl<sub>2</sub>), 35 µl of sterile H<sub>2</sub>O and 5ng plasmid DNA was added. Sample

mixture was incubated on ice for 20 min followed by 10 min incubation at room temperature, after which, 1 mL of LB medium was added followed by an incubation at 37 °C with 200 rpm shaking for 1h. Entire sample was inoculated in 10 mL of LB medium (Life Technologies) with kanamycin (50 µg/mL) and incubated overnight.

### **2.1.3- Recombinant protein induction**

Culture conditions (growth temperature, concentration of isopropyl-beta-D-thiogalactopyranoside (IPTG), addition of glucose and presence of iron salts in the culture) were evaluated to determine the optimal conditions for high protein yield. Analysis of recombinant protein production was done quantitatively using SDS-PAGE (stained by Coomassie Blue) and ChemiDoc imaging software (Biorad).

Different temperatures including room temperature (18 °C), 30 °C and 37 °C, were used to grow transfected *E. coli*. Supplementation with glucose to a concentration of 1% (w/v) in the medium was also tested.

Protein solubilisation from the membranes was also tested with the use of dodecylmaltoside (DDM) at controlled amounts.

### **2.1.4- Protein Purification**

Purification of SUMO-TAT-AOX was processed in collaboration with Liliya Euro from the University of Helsinki.

Recombinant protein purification was achieved by cell lysis followed by harvesting the soluble fraction. The obtained protein extracts were diluted in starting buffer (20 mM NaH<sub>2</sub>PO<sub>4</sub>, 500 mM NaCl and 20 mM Imidazole) and purified by affinity chromatography.

Briefly, a HIS trap F crude 5 mL (Life Technologies) was used to separate the recombinant protein from the rest of the extracts, resulting sample from the passing of the extract in starting buffer through the column was collected and labelled flow through (FT). Column was washed with 70 mM imidazole starting buffer, resulting sample from the wash was collected and labelled Fraction 1. A second wash of the column was performed with 200 mM imidazole starting buffer, resulting sample from the wash was collected and labelled Fraction 2. Purified recombinant protein was submitted to a process of desalting, using concentration columns (Vivaspin, Sartorius), by replacing the buffer (20 mM NaH<sub>2</sub>PO<sub>4</sub>, and 40 mM Imidazole). Separation of the SUMO from the recombinant AOX was performed using a SUMO protease (Life Technologies) according to the manufacturer's instructions.

A second purification was performed to separate the recombinant protein from the non-cleaved form and soluble SUMO protein. In summary, the cleavage product was

resuspended in starting buffer and passed through HIS trap F crude 5 mL, resulting sample from the passing of the cleavage product in starting buffer through the column was collected and labelled TAT-AOX. Column was washed with 200 mM imidazole starting buffer, resulting sample from the wash was collected and labelled SUMO.

All samples were analysed qualitatively by Western blot using an anti-AOX antibody, and quantitative by SDS-PAGE (stained by Coomassie Blue) and ChemiDoc imaging software (Biorad).

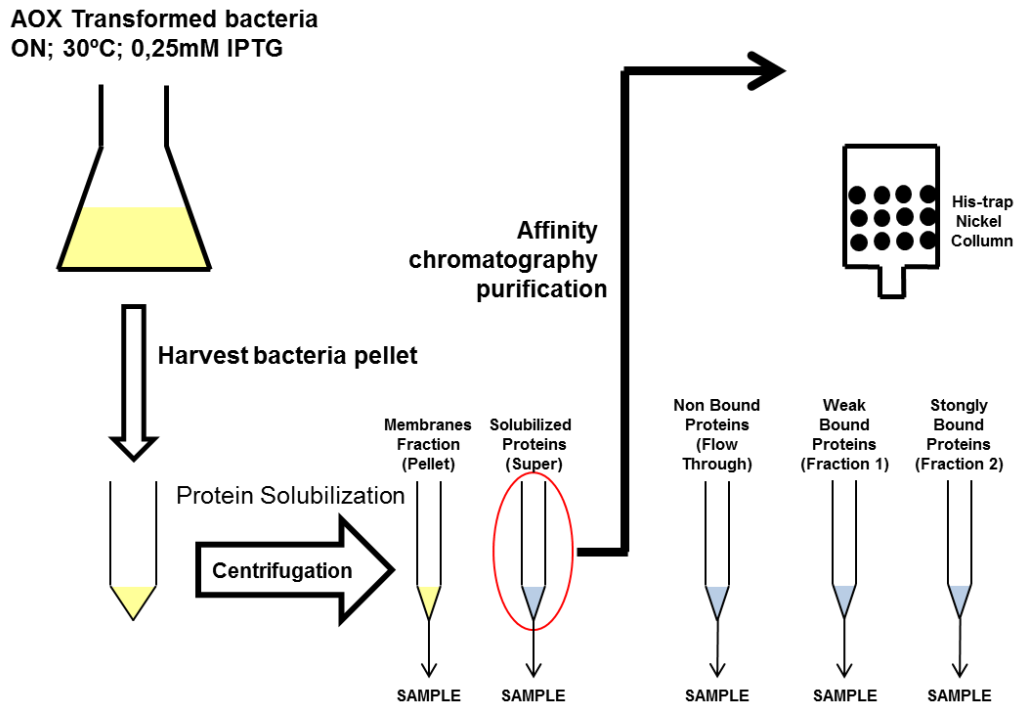


Figure 4 Scheme of protein purification

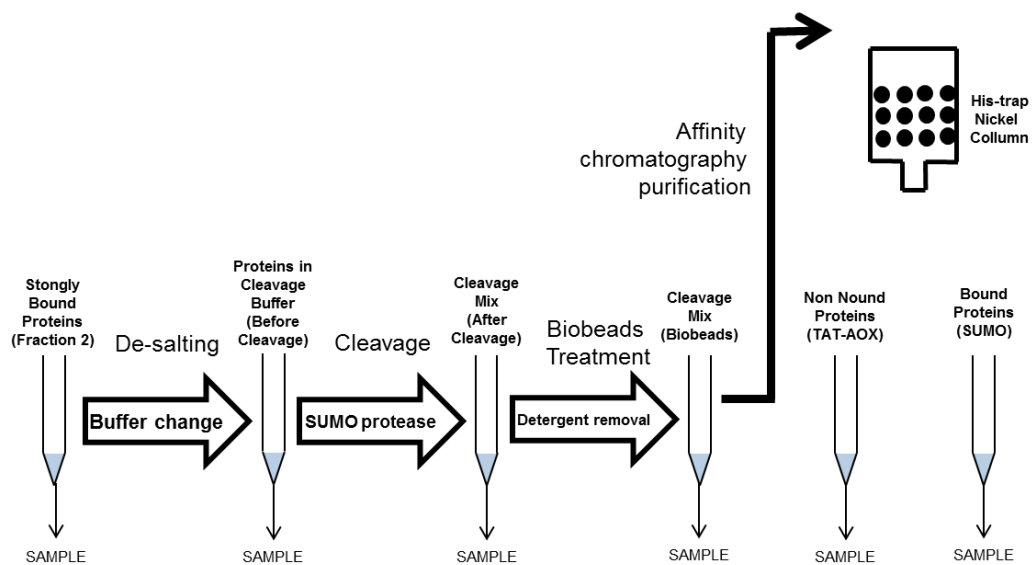


Figure 5 Scheme of SUMO cleavage and second TAT AOX purification

### **2.1.5- Recombinant AOX activity**

Recombinant TAT-AOX protein activity was evaluated by AMA (Sigma Aldrich) resistance selection. Briefly, 3T3 WT cells were seeded in 24-well plates and let grown until 60% confluency was reached. Growth medium was removed and the well was filled, up to one sixth of its total volume, with growth medium with 0.027 µg/µL of recombinant protein. Plates were incubated for 1 h at 37 °C, followed by addition of medium up to half of the volume of the well and incubated for 3 h. AMA was added to a concentration of 100 µM and incubated for 48 h. Protein activity was determined by the presence and number of living cells in the culture in comparison with controls (3T3 WT and 3T3 AOX in the same conditions).

Complementary *ex vivo* assays were done by Natascha Sommer in Giessen (Germany) using the perfused lung from littermate wild type (WT) with simulation of hypoxia, and measuring the variation in the pulmonary arterial pressure (PAP) when the lung was submitted to hypoxia and perfused with physiological buffers containing recombinant AOX protein. Controls were lungs from *Aox<sup>Rosa26</sup>* and WT littermates.

## **2.2- AOX protection against CSE damage**

### **2.2.1- Cell lines**

Mouse embryonic fibroblast cells (MEFs) were isolated, by Praven Kumar (University of Helsinki), from embryos expressing AOX and their WT littermate as a negative control. Immunostaining confirmed expression of AOX. Primary cells were immortalized using a recombinant lentiviral vector<sup>(53)</sup>.

Eric Dufour (University of Tampere) generated 293T Human Embryonic Kidney cells (HEK) and NIH 3T3 fibroblast expressing AOX or GFP as described by Hakkaart et al. (2006)<sup>(7)</sup>. Briefly, the cells were virus transfected using an AOX vector with a green fluorescent protein (GFP) marker, positive transfection was evaluated by GFP detection using a fluorescence microscopy. All cell lines used were tested for AOX expression by Western blot using a specific AOX antibody.

### **2.2.2- CSE production**

CSE was produced by bubbling smoke of a research cigarette<sup>(54)</sup> (3R4F, 0.7 mg nicotine and 9.5 mg tar, University of Kentucky Tobacco Research and Development

Centre), through 10 mL of cell growth medium using a peristaltic pump (Langer Instruments) for suction. The cigarette was smoked within 1 min. The CSE (stock) was then filter-sterilized using a 0.22 µm nylon filter (Sigma Aldrich), followed by a quality control analysis by measuring the pH and OD at 320 nm for standardization (pH 7.4; OD<sub>320nm</sub> = 0.7).

### **2.2.3- Cell counting and seeding**

Cells were grown in a 10 cm plate until reaching a 80% confluency, then trypsinised and pelleted in a 10 mL plastic vial by spinning at 800 rpm for 3 min. Pellet was re-suspended in 1 mL sterile PBS and counted using a Bürker chamber. Equal number of cells (25 000) was seeded into 24-well plate to ensure the same quality and quantity of cells on day of experiment.

### **2.2.4- Plate-coating**

Coated plates were prepared by covering the bottom surface of the well with a coating agent, and incubated in a cell culture hood at room temperature for 30 min. Excess of coating agent was washed off using sterile 1X phosphate buffered saline (PBS). Two different coating agents, 5% (w/v) gelatine solution (Millipore) and 0.1% (w/v) polylysine solution (Life Technologies), were used to produce different coated plates.

### **2.2.5- Growth mediums**

Different cell culture media were used to test different metabolic conditions: (a) Dulbecco's Modified Eagle's medium (DMEM) with high glucose (25 mM) (Lonza), (b) DMEM with low glucose (5 mM) (Lonza) and (c) DMEM with galactose (10 mM) (Life technologies). Cell cultures were grown in an incubator chamber maintained at 37 °C with a CO<sub>2</sub> saturation level of 5%.

Medium supplements used were 1x Glutamax (Life Technologies), 1x Penstrep (Life Technologies), Fetal Bovine Serum (FBS) (Life Technologies), 1mM sodium pyruvate (Sigma Aldrich) and Calf Bovine Serum (CBS) (ATCC), according to Table 1.

**Table 1** Details of medium supplements and serum concentration for each cell type used.

DMEM	SERUM	SUPPLEMENTS	CELL TYPE USED
HIGH GLUCOSE	20% FBS	Glutamax and Penstrep	MEFs
HIGH GLUCOSE	10% FBS	Glutamax and Penstrep	HEK
HIGH GLUCOSE	10% CBS	Glutamax and Penstrep	3T3
LOW GLUCOSE	10% FBS	Glutamax and Penstrep	HEK
LOW GLUCOSE	5% FBS	Glutamax and Penstrep	MEFs
LOW GLUCOSE	10% CBS	Glutamax and Penstrep	3T3
GALACTOSE	20% FBS	Sodium pyruvate and Penstrep	MEFs
GALACTOSE	10% FBS	Sodium pyruvate and Penstrep	HEK
GALACTOSE	5% FBS	Sodium pyruvate and Penstrep	MEFs
GALACTOSE	10% CBS	Sodium pyruvate and Penstrep	3T3

Galactose medium were not supplemented with glutamax since the medium formulation already contained glutamine. Sodium pyruvate supplementation was necessary in order to correlate the physiological response with the high and low glucose medium, which had a 1 mM concentration in their formulation.

### **2.2.6- Exposure to CSE**

Cell cultures with a confluence between 60% were incubated with CSE at different concentrations (prepared by diluting the stock CSE with growth medium). Cells were incubated for 24h or 48h to measure the effect of toxins over time.

### **2.2.7- Evaluation of response mechanisms**

Cell plates were analysed using a cell viability kit (Cell Counting Kit 8, Sigma Aldrich). Briefly, cells were washed with 1x PBS (Life Technologies) followed by incubation with Dulbecco's Phosphate Buffered Saline (DPBS) medium (Life Technologies) with 2% (v/v) of reagent from the kit. Absorbance at 450 nm estimated the number of viable cells by using a calibration curve. Statistical correlation by ANOVA two-way test was used to evaluate the differences in the physiological response to CSE exposure between the AOX expressing cells and its controls.

## 3- Results

### 3.1- Purification of catalytically active recombinant AOX

The first goal of this work was to produce and purify an active AOX in heterologous systems. To achieve this different approaches were used to increase the yield of AOX protein production in transformed bacteria. Soluble recombinant protein produced was purified and tested for integration and catalytic active in mammalian cells.

#### 3.1.1- Recombinant AOX production in bacteria

Transformed bacteria *E.coli* BL21 showed to be viable and proliferative at 37 °C, with a slower growth rate in culture induced with addition of IPTG, comparatively to non-induced cultures, thus suggesting that a metabolic extra burden, such as the recombinant AOX production, was slowing down their growth rate (Figures 4-1 and 5-1), such behaviour is common when inducing recombinant protein production in *E.coli*<sup>(55)</sup>. Furthermore, SDS-Page analysis of different time points after induction provided evidence that recombinant AOX was actually being expressed, by the appearance of a band approximately 60 kDa in the induced culture, which was absent before induction (Figures 4-2 and 5-2).

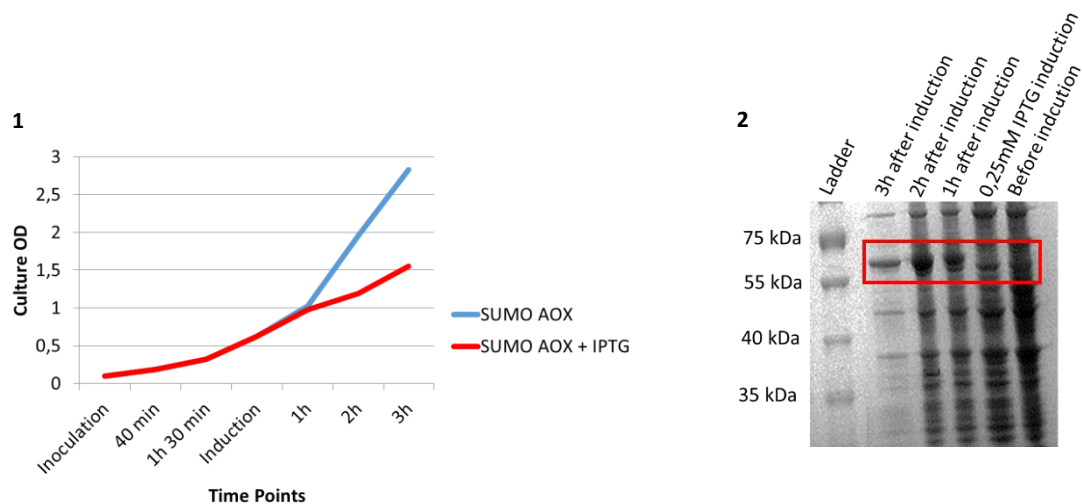


**Figure 6** SUMO AOX production analysis: growth monitoring by OD<sub>600</sub> measurement in specific time points (1) and SDS-Page analysis of samples harvested in specific time points with location of SUMO TAT-AOX (approximately 60 kDa) is highlighted in red box. (2)

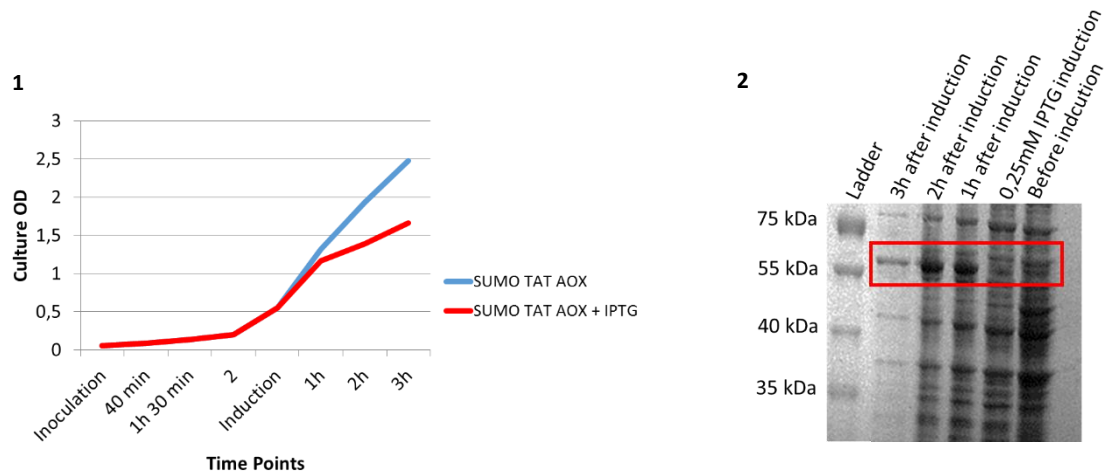


**Figure 7** SUMO TAT-AOX production analysis: growth monitoring by OD<sub>600</sub> measurement in specific time points (1) and SDS-Page analysis of samples harvested in specific time points with location of SUMO TAT-AOX (approximately 60 kDa) is highlighted in red box. (2).

### 3.1.2- Increasing yield of protein in soluble form

To increase the amount of protein in the soluble fraction, in order to simplify the extraction and purification from the bacterial culture, overnight growth in transformed *E. coli* BL21 (DE3) at room temperature (RT), 30 °C and 37 °C was analysed (Figure 6), to determine if by reducing the growth temperature, thus slowing down culture growth, to values bellow the optimal 37 °C, could increase the accumulation of soluble protein. It was possible to observe that the difference between the amount of protein in the soluble fraction and in the membrane fraction was smaller when cells were grown at 30 °C (ratio 1:1.5) when compared to growth at RT (ratio 1:2.5) and 37 °C (ratio 1:2.4).

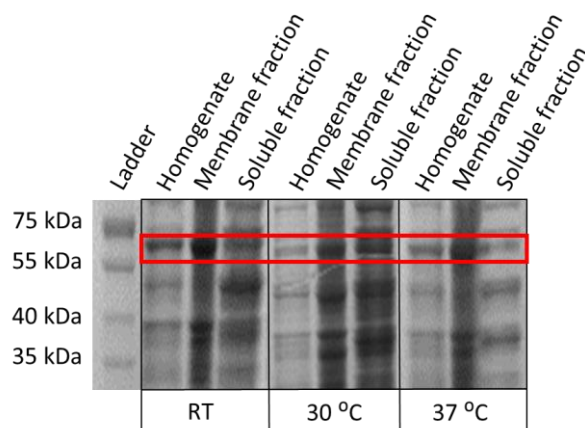


**Figure 8** SDS-Page of SUMO TAT-AOX production analysis of homogenate, membrane fraction and soluble fraction at different growth temperatures: room temperature (RT), 30 °C and 37 °C. Location of SUMO TAT-AOX (approximately 60 kDa) is highlighted in red box.

In combination with decreasing the growth temperature to 30 °C, different strengths of protein induction were tested, by decreasing the concentration of the pET30 system inducer (IPTG) in the growth medium. SDS-Page analysis showed that decreasing the IPTG concentration did not increase the yield of soluble protein (ratio 1:1,5), furthermore IPTG induction with concentrations lower than 0.005 mM were not able to induce recombinant protein expression (Figure 7-1). Addition of glucose to the growth medium did not increase the yield of soluble protein, thus proving that the low yield was not due to a low expression of the protein by the promoter sequence in the plasmid<sup>(56)</sup> (Figure 7-2).

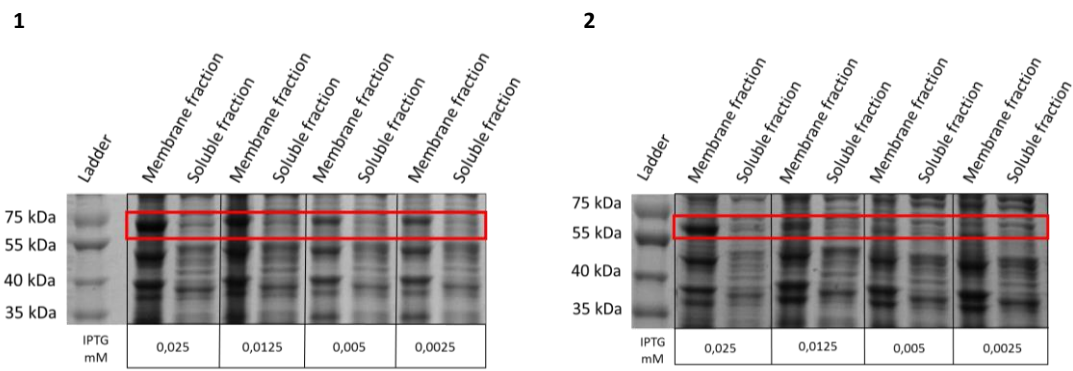


**Figure 9** SDS-Page of SUMO TAT-AOX production analysis of membrane fraction and soluble fraction at grown at 30 °C with different IPTG induction in LB with kanamycin (1) and LB 1% glucose with kanamycin (2). Location of SUMO TAT-AOX (approximately 60 kDa) is highlighted in red box.

Due to the low yield after the change in growth condition, solubilisation of the protein incorporated in the membrane fraction was performed using DDM. Solubilisation of the entire amount of protein was not achieved, however an increase in the amount of soluble protein (from 1:1.5 to 1:0.45, Figure 8) was observed, upon using a 1.5% (w/v) DDM concentration. Despite the promising result one cannot overlook the fact that harsh solubilisation treatments, such as the one performed, can compromise the recombinant protein catalytic activity<sup>(57)</sup>, thus rendering it useless for the delivering of a catalytically active protein to the cells.

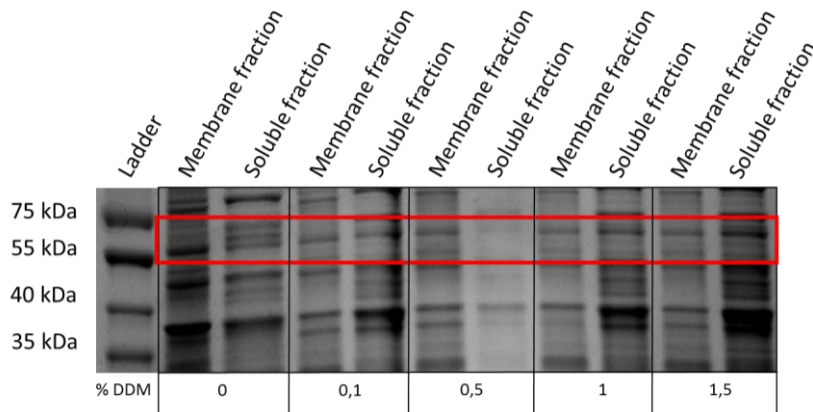


**Figure 10** SDS-Page of SUMO TAT-AOX analysis of membrane fraction and soluble fraction with protein solubilisation using different DDM concentrations. Location of SUMO TAT-AOX (approximately 60 kDa) is highlighted in red box.

Since in *E. coli* BL21 (DE3) the accumulation of recombinant protein tended to be higher in the membrane fraction than in the soluble fraction, another *E. coli* strain was used for the protein production. By repeating the temperature and IPTG tests in transformed *E. coli* Rosetta 2, a shift in the distribution of the protein between the soluble fraction and the membrane fraction was achieved (from Figure 9), when grown overnight at 30 °C (ratio 1:1) in opposition to growing overnight at 37 °C (ratio 1:1.5) .

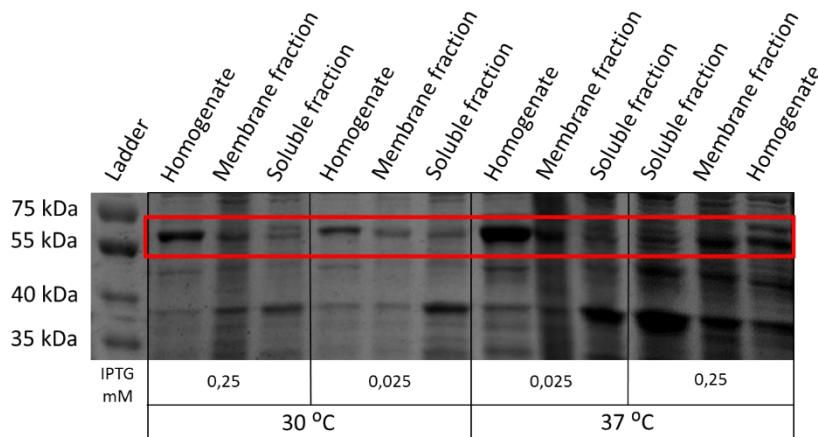


**Figure 11** SDS-Page of SUMO TAT-AOX production analysis of homogenate, membrane fraction and soluble fraction at 30 °C and 37 °C with 0,25mM IPTG and 0,025mM IPTG. Location of SUMO TAT-AOX surrounded at red.

In order to understand why most of the protein was being incorporated into the membranes, despite the conjugation of SUMO protein, an analysis of the protein structure was performed. After obtaining a 3D structural model for the *Ciona intestinalis* AOX protein (designed by Liliya Euro), it was possible to identify the influence of the di-iron II active centre.

Effect of iron salts supplementation was tested by performing a SDS-Page analysis of transformed *E. coli* Rosetta 2 grown at 30 °C with a 0.25 mM IPTG induction and with different concentrations of iron II (Fe2) and iron III (Fe3) supplementation in the growth medium, respectively. In both, Fe2 and Fe3 supplementation a clear increase of protein in the membrane fraction with the increase in iron concentration in the medium was achieved (Figure 10).

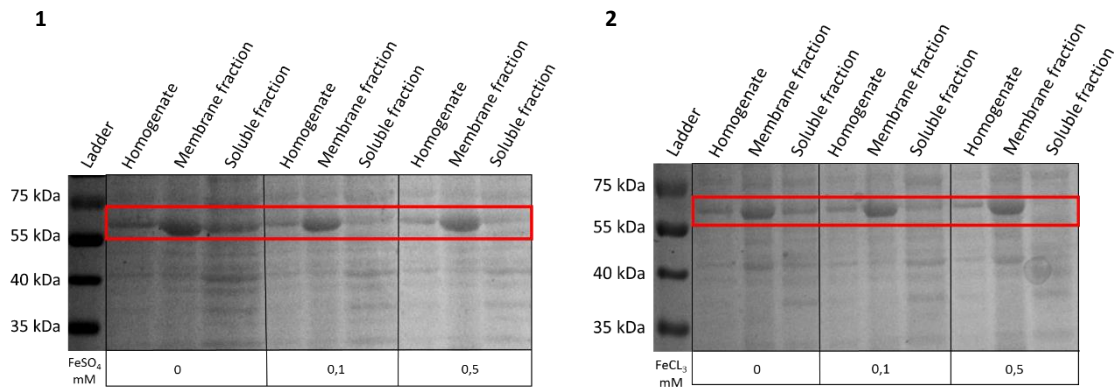


**Figure 12** SDS-Page of SUMO TAT-AOX production analysis of homogenate, membrane fraction and soluble fraction grown at 30 °C in LB kanamycin medium with iron II supplementation (1) and iron III supplementation (2). Location of SUMO TAT-AOX surrounded at red.

### 3.1.3- Purification of recombinant AOX

Purification of recombinant AOX from bacterial extract was performed by using a HIS trap affinity chromatography purification technique, which targeted the SUMO protein’s HIS tag. Despite being able to successfully target the recombinant protein (Figure 11), imidazole presence in the buffer seemed to be crucial to keep the protein soluble in order to perform the cleavage of the SUMO protein (Figure 12 and 13).

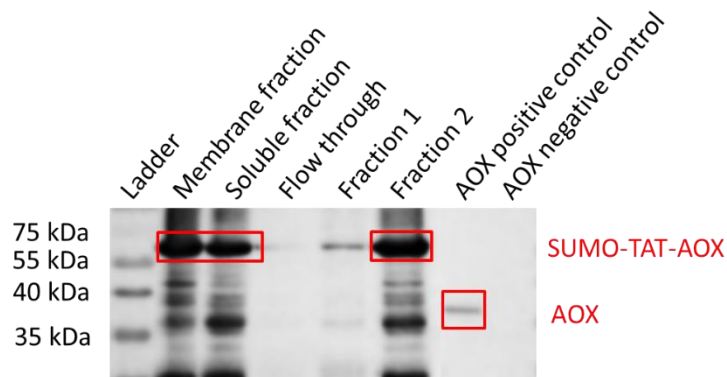


**Figure 13** Western blot of SUMO-TAT-AOX HIS trap affinity chromatography purification results. Red rectangles highlight locations of SUMO-TAT-AOX (approximate 60 kDa) and AOX (approximate 37 kDa)

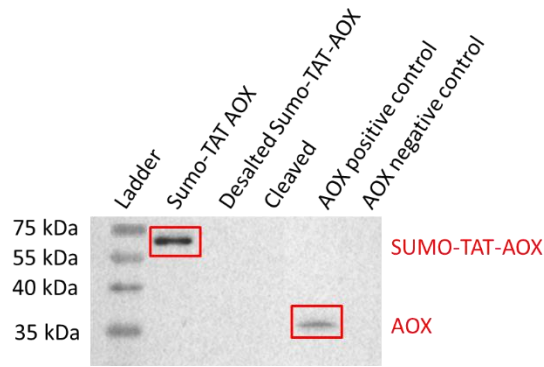


**Figure 14** Western blot of SUMO-TAT-AOX desalting and SUMO cleavage (cleaved) results. Red rectangles highlight locations of SUMO-TAT-AOX (approximate 60 kDa) and AOX (approximate 37 kDa)

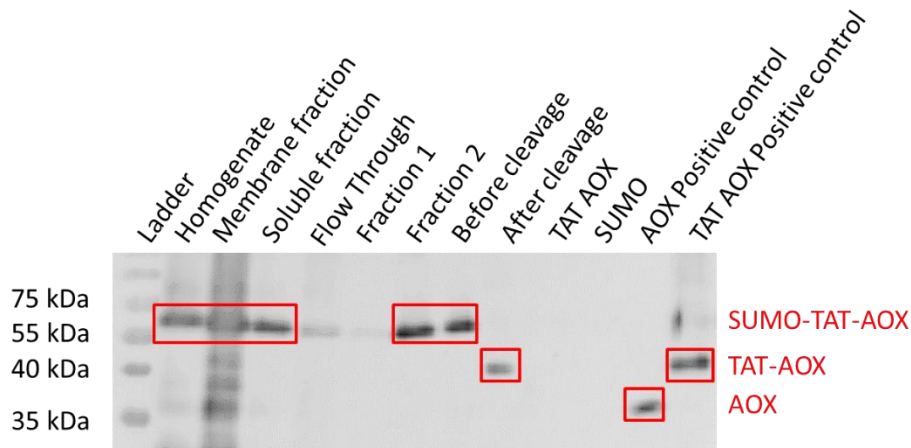


**Figure 15** Western blot of SUMO-TAT-AOX purification protocol results, using imidazole in the desalting step (before cleavage) and attempting to purify TAT-AOX from the other proteins in the cleavage product. Red rectangles highlight locations of SUMO-TAT-AOX (approximate 60 kDa), TAT-AOX (approximate 40 kDa) and AOX (approximate 37 kDa).

Although it was possible to produce an enriched TAT-AOX extract (containing the TAT-AOX, SUMO protein and other unidentified bacterial proteins), the production of a purified TAT-AOX extract proved to be challenging due to the loss of recombinant protein in the second purification, which was aimed to separate TAT-AOX from the other proteins in the extract. Nonetheless the enriched TAT-AOX extract was used to analyse the catalytic activity and cell delivery of the purified TAT-AOX.

### 3.1.4- Recombinant AOX activity

*In vitro* assays to test the activity of the recombinant AOX were performed by adding enriched TAT-AOX extract to the growth medium of a 60% confluent NIH 3T3 cell plate and incubation for 3 h, followed by addition of 100  $\mu$ M AMA and incubation for 48 h at 37 °C. It was observed, both visually and quantitatively, that the culture exposed to the recombinant protein showed a significant difference in number of viable cells to the non-exposed culture ( $p < 0.05$ , Figure 14 and 15). Furthermore, AMA resistance conferred by the addition of enriched TAT-AOX extract, correlated to the AMA resistance present in the AOX cell lines used as control.

Cell proliferation in control conditions after exposure to TAT-AOX (visual observation of a culture with 90% confluence) was found to be much lower than in non-exposed cells (over confluent), this significant difference in number of viable cells in controlled condition ( $p < 0.05$ ; Figure 15). Recombinant protein concentrations higher than 0.027  $\mu$ g/ $\mu$ L lead to the death of the entire culture, in a period less than 3 h. TAT-AOX transfection success (40%-50%), in exposed cells was visually estimated, with correlation to the ratio obtained in the quantification, by comparing the amount of viable cells after 48 h AMA incubation. In summary, there was evidence that the purified TAT-AOX was active and incorporated into the cells, however the enriched TAT-AOX extract seemed to have certain degree of toxicity to mammalian cells.

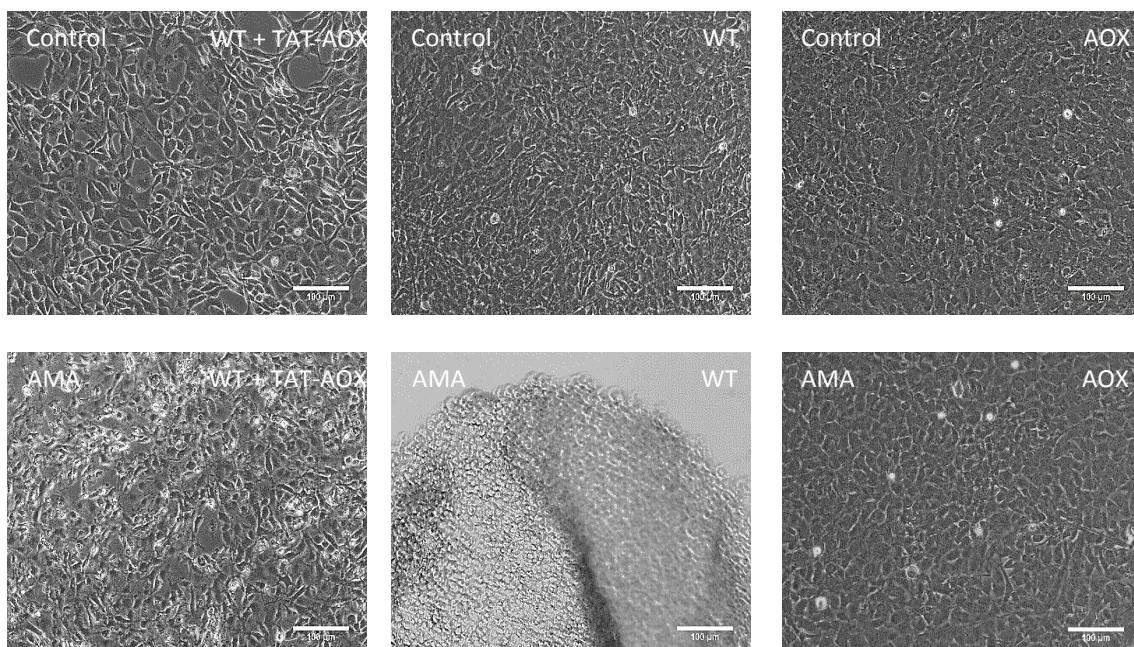


**Figure 16** *In vitro* TAT-AOX activity results of AMA incubation in NIH 3T3 cell lines: *wild type* (WT), AOX and *wild type* with TAT-AOX diluted in growth medium (WT+TAT-AOX). Dead cells appear as round and bright cells.

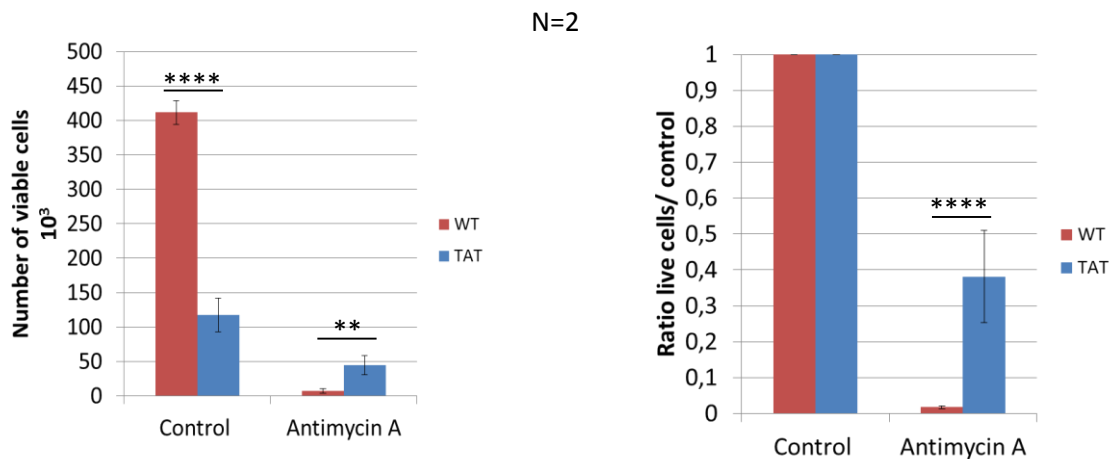


**Figure 17** Results of NIH 3T3 WT and exposed to enriched TAT-AOX (TAT), incubated in DMEM with 100  $\mu$ M AMA for 48 h, in both number of thousands of viable cells (on the left) and ratio between live cells in tested condition and control condition with no AMA (on the right). Significance of the difference in the measured values is represented by the stars (\*), the more stars represented the higher the significance

*Ex-vivo* activity assays of the enriched TAT-AOX extract, were performed by Natascha Sommer's laboratory (Giessen, Germany), using a WT perfused lung. To correlate any obtained results to the recombinant protein activity, the physiological response to hypoxia of perfused lungs of both WT and AOX<sup>rosa26</sup> littermate mice were analysed to serve as a negative and positive control, respectively. It was reported that WT perfused lungs, had an elevated variation of PAP, under the first hypoxic challenge, which was attenuated by the increase of O<sub>2</sub> concentration in the perfusion buffer (unpublished results). Oppositely, AOX had a low variation of PAP under the first hypoxic challenge time points, which increased with the increased O<sub>2</sub> concentration in the perfusion buffer up to an O<sub>2</sub> concentration of 1:1000, followed by an attenuation of the variation of PAP with further increase O<sub>2</sub> concentration (unpublished results). Both lungs used in the experiment showed similar physiological behaviour under perfused weighted (PW) normoxia and under hypoxia (HOX) conditions (unpublished results). Furthermore, both lungs were responsive to U46<sup>(58, 59)</sup> (pharmacological compound that induces vasoconstriction) induced hypoxia conditions, showing an elevated variation of PAP.

Perfusion of a WT lung under HOX condition, with physiological buffer containing a dilution of the enriched TAT-AOX extract, achieved a nullification in hypoxia variation of PAP (Figure 16), which correlated to the physiological response of a perfused AOX lung. The used WT lung was responsive to U46 induced hypoxia conditions, by showing an elevated variation of PAP.

Hypoxic pulmonary vasoconstriction is a self-regulatory mechanism, responsible for an increase in PAP value under low O<sub>2</sub> availability (hypoxia) <sup>(60)</sup>. Therefore, information regarding the lung response to HOX can be obtained by analysing the variation of PAP.

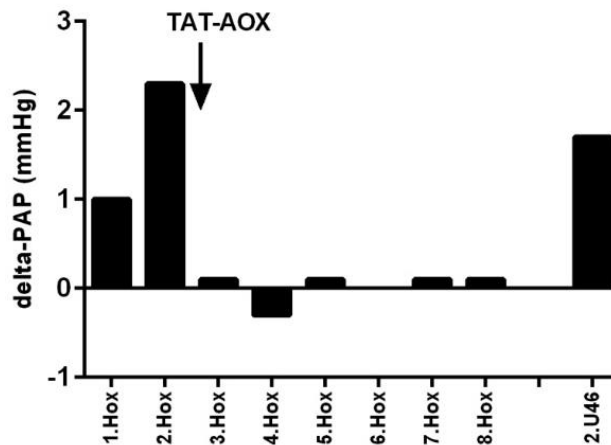


**Figure 18** *Ex vivo* TAT-AOX activity results of perfusion of a WT lung with TAT-AOX (point of perfusion indicated by arrow) in physiological buffer. This figure is shown with the permission of Natascha Sommer.

### 3.2- AOX protection against CSE damage

In order to investigate if AOX expression in the mitochondria's respiratory chain could confer some degree of protection against damaged caused by CSE, physiological response of AOX transgenic cell lines to exposure of CSE dilutions for 24h and 48h respectively, was analysed. WTs of each cell line were used as a control. In the tested fibroblast cell lines, AOX and WT were identical with respect to cell morphology as well as growth rate. To favour different metabolic conditions, different DMEM media were used. After exposure, the numbers of viable cells were quantified and normalized using a ratio of the number of viable cells in the tested CSE dilution to the number of viable cells in a control condition (same exposure time in growth medium without CSE).

#### 3.2.1- 293T HEK cells

293T HEK cells are known to detach easily from plates. During the experiments, a difference between the numbers of cells in the wells, immediately after replacing the growth medium with diluted CSE medium was observed, thus generating a well-to-well error in the quantification of viable cells. An alternative was to apply coating agents to

avoid of the loss of cells. In such conditions when the coating agents (gelatine and polylysine) were applied to the plates before seeding the cells a decrease in the amount of lost cells (visual estimation of approximately 30%) was observed, nonetheless the detachment of a considerable amount of cells upon replacing growth medium was still present in the assay, therefore all measurements performed had a well-to-well error.

From several attempts made to perform the experiments, only one set of experiments, using polylysine coating treatment, produced a quality result where the loss of cells was consistent across all wells (visual estimation of approximately 10%-15%). In these experiments HEK cell lines were able to remain viable when incubated for 24h in CSE concentrations up to 30%. Number of viable cells decreasing with the increase in CSE concentration. Concentrations higher than 30% lead to the death of entire culture in both cell lines.

Upon quantifying the number of viable cells after a CSE long-term incubation (24 h) in DMEM supplemented with 10% FBS (low glucose and galactose), no significant difference in the viable cell quantity between the AOX and WT cell lines was detected ( $p>0.05$ ; Figures 17 and 18), thus suggesting that there is no difference in physiological response to CSE between AOX and WT. Due to the inability to eradicate or nullify the well-to-well error in the experiments, further testing with this cell line were stopped, in favour of other cell lines more adherent to the plate surface, such as fibroblast cell lines (MEFs and NIH 3T3).

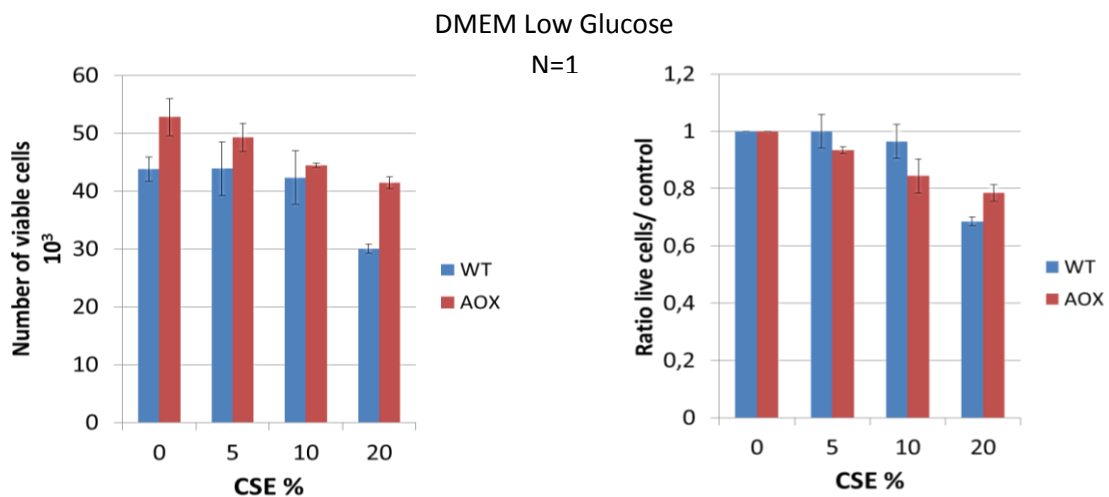


**Figure 19** Results of HEK cells incubated in CSE dilutions in DMEM low glucose for 24 h in both number of thousands of viable cells (on the left) and ratio between live cells in tested condition and control condition with 0% CSE (on the right).

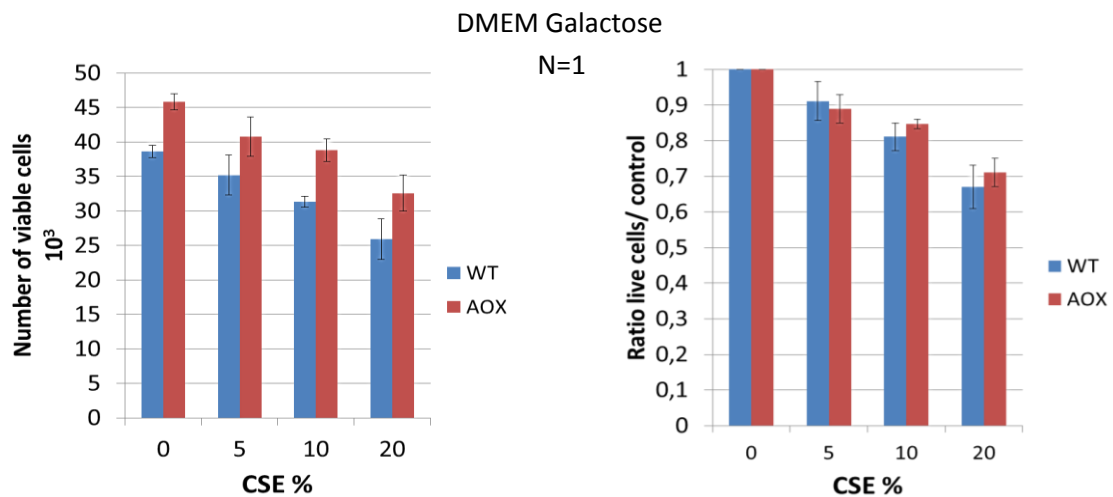


**Figure 20** Results of HEK cells incubated in CSE dilutions in DMEM galactose for 24 h in both number of thousands of viable cells (on the left) and ratio between live cells in tested condition and control condition with 0% CSE (on the right).

### 3.2.2- MEFs from Aox-Rosa26

In the experiments performed with MEFs cell lines (both AOX and WT), cells were able to remain viable when incubated for 24 h in CSE-supplemented media with CSE concentrations up to 8%. Number of viable cells decreased with increasing concentrations of CSE. Concentrations higher than 8% lead to the death of entire culture in both cell lines.

Upon quantifying the number of viable cells after a CSE long-term incubation (24 h and 48 h) in DMEM supplemented with 20% FBS (low glucose and galactose), no significant difference in the viable cells quantity between the AOX and WT cell lines was observed ( $p > 0.05$ ; Figures 19 and 20), thus suggesting that there is no difference in physiological response to CSE between AOX and WT.

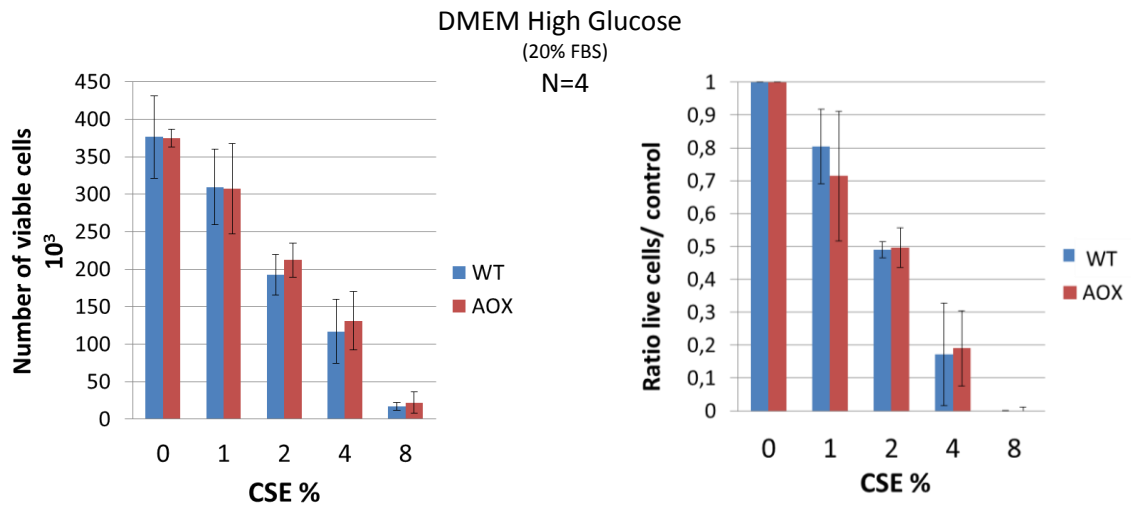


**Figure 21** Results of MEF cells incubated in CSE dilutions in DMEM high glucose for 48 h in both number of thousands of viable cells (on the left) and ratio between live cells in tested condition and control condition with 0% CSE (on the right).

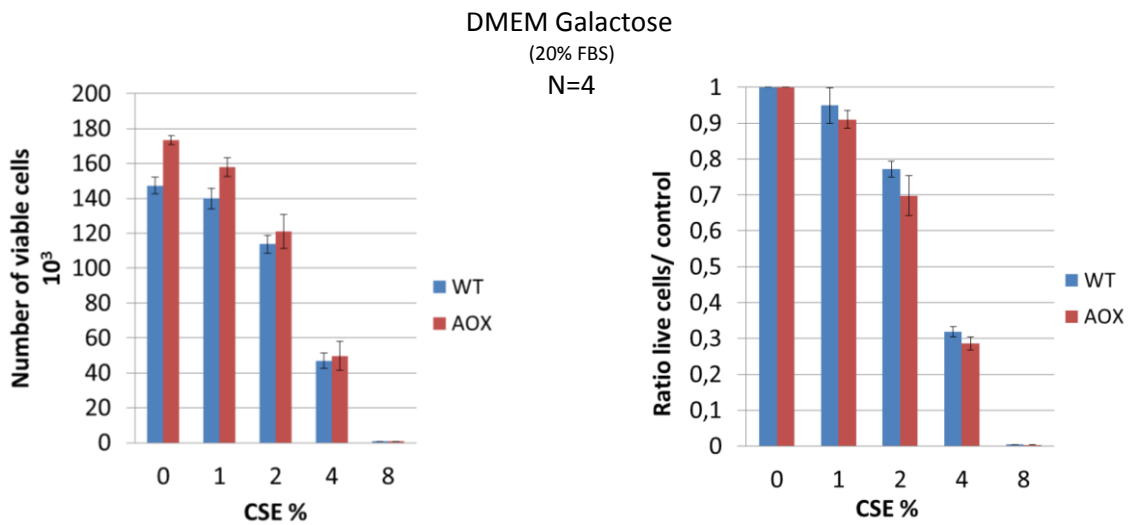


**Figure 22** Results of MEF cells incubated in CSE dilutions in DMEM galactose for 48 h in both number of thousands of viable cells (on the left) and ratio between live cells in tested condition and control condition with 0% CSE (on the right).

After the first set of experimental analysis, it was determined that higher amounts of FBS in the medium could eventually provide a protective effect to the cells from CSE, thus masking AOX protection. To assure that experimentally, a deadly blockade at the complex III level, was induced by overnight incubation of cell cultures in 20% FBS DMEM (high glucose) with 100  $\mu$ M AMA. Both of the cell lines were able to remain viable after AMA exposure, as opposite to what was expected since AMA should have produced a

lethal effect in the WT lines, which were unable to bypass the induced blockade. As a secondary validation, the same AMA treatment was performed using DMEM medium supplemented with 5% FBS (instead of 20% FBS). After the overnight incubation the, WT cell's survival was greatly compromised in comparison to the AOX, which were still able to proliferate after removing the AMA.

With this new data the same CSE incubation experiment was performed, using DMEM medium supplemented with 5% FBS to determine if the absence of a protective effect was indeed due to the high concentration of FBS. CSE concentration in which cells were able to remain viable was decrease to concentrations up to 5%, when comparing to the 8% CSE concentration in the previous CSE incubation experiments

By quantifying the number of viable cells after a CSE long-term incubation of 24 h in DMEM (low glucose and galactose), no significant difference in the viable cells quantity between the AOX and WT cell lines was detected ( $p>0.05$ ; Figures 21 and 22). Same result was observed with a CSE incubation of 48 h in DMEM galactose ( $p>0.05$ ; Figure 23), thus suggesting that there is no difference in physiological response to CSE between AOX and WT.

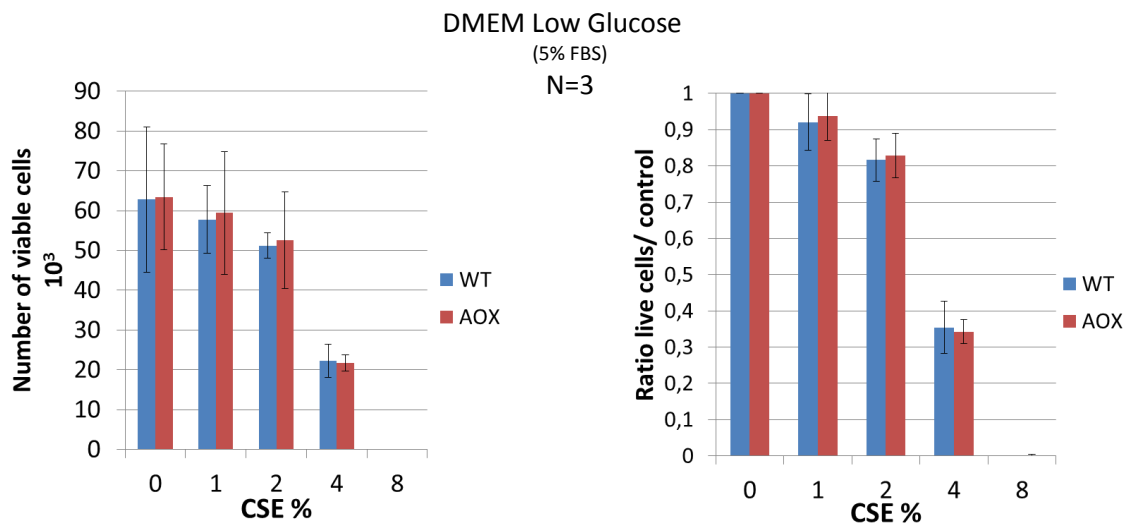


**Figure 23** Results of MEF cells incubated in CSE dilutions in DMEM low glucose (5%FBS) for 24 h in both number of thousands of viable cells (on the left) and ratio between live cells in tested condition and control condition with 0% CSE (on the right).

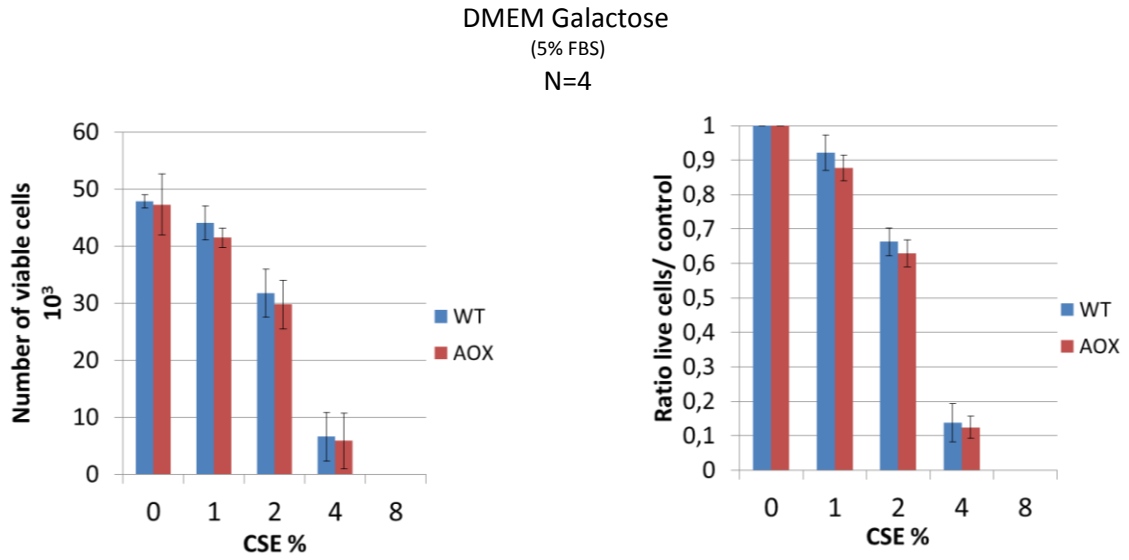


**Figure 24** Results of MEF cells incubated in CSE dilutions in DMEM galactose (5%FBS) for 24 h in both number of thousands of viable cells (on the left) and ratio between live cells in tested condition and control condition with 0% CSE (on the right).

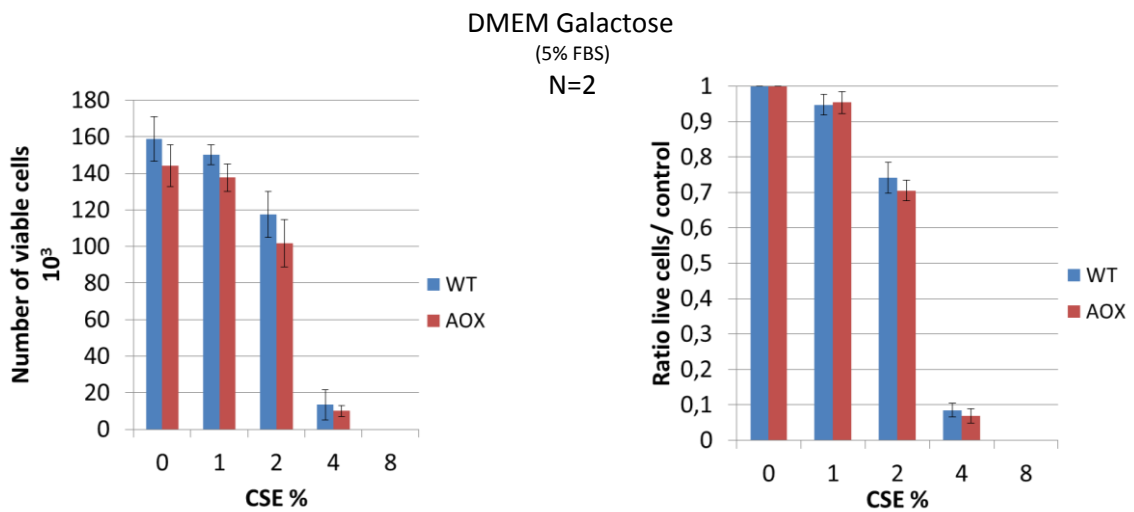


**Figure 25** Results of MEF cells incubated in CSE dilutions in DMEM galactose (5%FBS) for 48 h in both number of thousands of viable cells (on the left) and ratio between live cells in tested condition and control condition with 0% CSE (on the right).

In order to analyse if the absence of a protective effect was due culture growth being desynchronized, a long term CSE incubation (48 h) with the addition of a 24 h DMEM 2% FBS incubation prior to CSE exposure, to synchronize the culture G0 phase by serum restriction<sup>(61)</sup>, was performed. By quantifying the number of viable cells no significant difference in the viable cell quantity between the AOX and WT cell lines was detected ( $p>0.05$ ; Figures 24), thus suggesting that there is no difference in physiological response to CSE between AOX and WT.

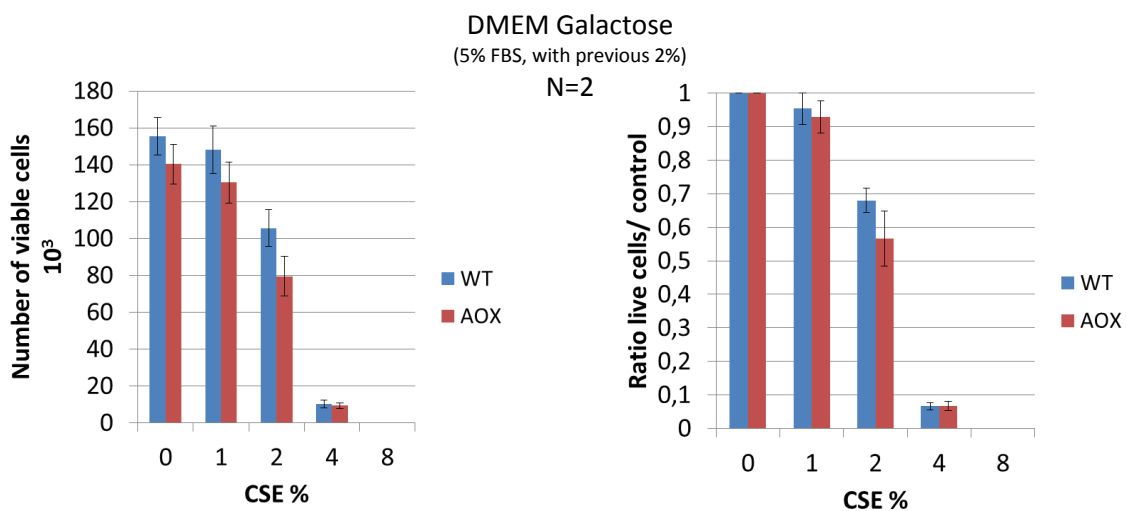


**Figure 26** Results of MEF cells incubated in CSE dilutions in DMEM galactose (5%FBS) for 48 h, with previous 24 h incubation in the same medium with 2% FBS, in both number of thousands of viable cells (on the left) and ratio between live cells in tested condition and control condition with 0% CSE (on the right).

### 3.2.3- NIH 3T3 cells

Upon the generation NIH 3T3 (both AOX and WT), a long term CSE incubation for 24 h using DMEM supplemented with 10% CBS (low glucose and galactose) was performed. A long term CSE incubation for 48 h using DMEM supplemented with 10% CBS (galactose) was also performed with and without culture synchronization by 24 h incubation in DMEM supplemented with 2% CBS before CSE exposure.

By quantifying the number of viable cells after a 24 h CSE long-term incubation in DMEM (low glucose and galactose), no significant difference in the viable cells quantity between the AOX and WT cell lines was detected ( $p>0.05$ ; Figures 25 and 26). Same result was also observed with a CSE long term incubation of 48 h in DMEM galactose, without and with the 2% CBS incubation ( $p>0.05$ ; Figure 27 and 28), thus suggesting that there is no difference in physiological response to CSE between AOX and WT.

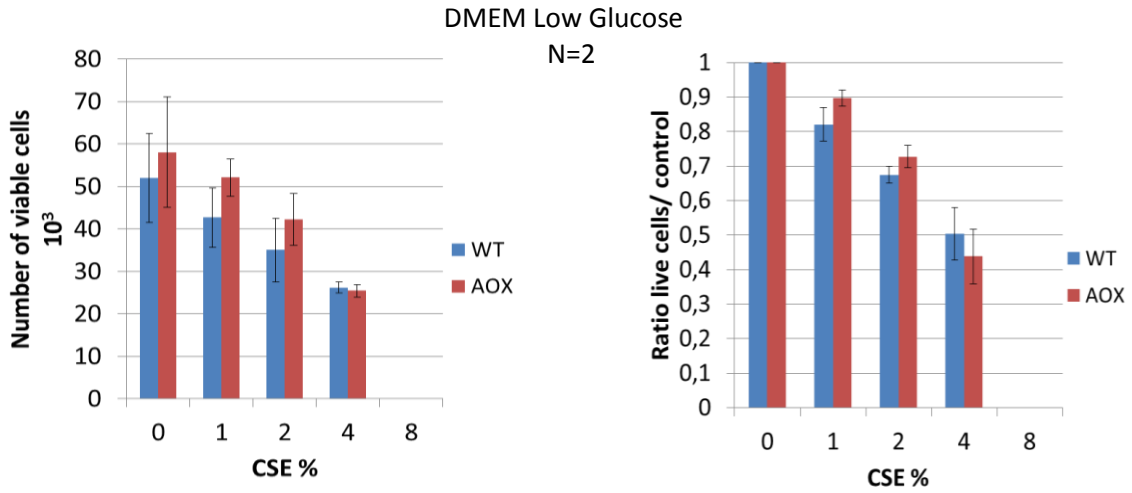


**Figure 27** Results of NIH 3T3 cells incubated in CSE dilutions in DMEM low glucose for 24 h, in both number of thousands of viable cells (on the left) and ratio between live cells in tested condition and control condition with 0% CSE (on the right).

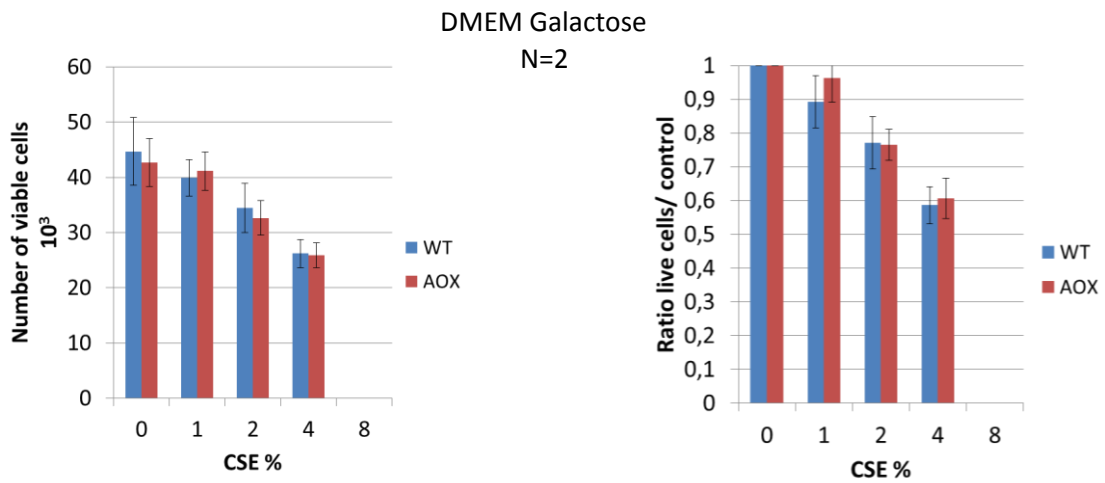


**Figure 28** Results of MEF cells incubated in CSE dilutions in DMEM galactose for 24 h, in both number of thousands of viable cells (on the left) and ratio between live cells in tested condition and control condition with 0% CSE (on the right).

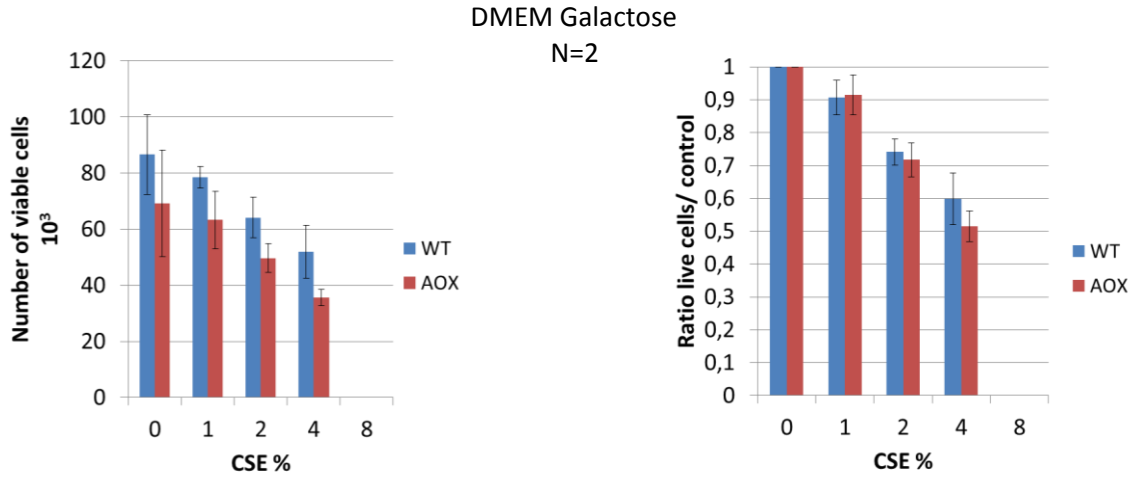


**Figure 29** Results of MEF cells incubated in CSE dilutions in DMEM galactose for 48 h, in both number of thousands of viable cells (on the left) and ratio between live cells in tested condition and control condition with 0% CSE (on the right).

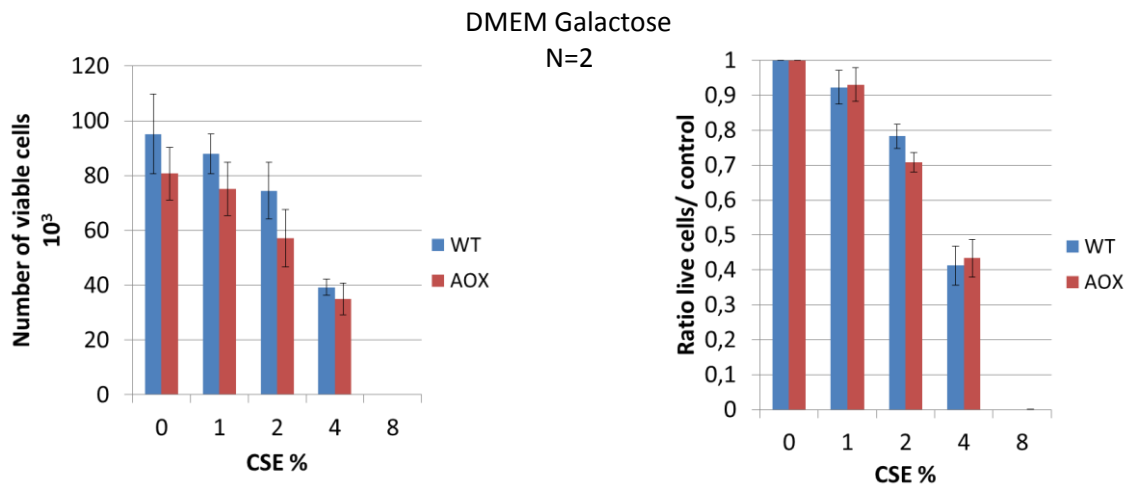


**Figure 30** Results of MEF cells incubated in CSE dilutions in DMEM galactose for 48 h, with previous 24 h incubation in the same medium with 2% FBS, in both number of thousands of viable cells (on the left) and ratio between live cells in tested condition and control condition with 0% CSE (on the right).

## 4- Discussion

In this work the first goal was to purify a catalytic active AOX protein in a heterologous system. Second goal was to test if AOX presence could be used to protect against cell damage caused by CSE. The combination of the results from both goals would provide a viable method to deliver a functional AOX inside the cells for medical treatment and data about AOX potential as an attenuation treatment of the cigarette smoke damage. Regarding the first goal, purified recombinant AOX from a bacterial extract was catalytically active and actively taken up by mammalian cells. On the second goal it was observed that AOX expression does not confer resistance to CSE.

### 4.1- Recombinant AOX production

Recent studies have provided promising results regarding the of AOX as a rescue treatment for patients with COX deficiencies <sup>(3, 4, 6)</sup>, therefore the question of how to deliver a catalytically active AOX to patients' cells was raised. Both messenger ribonucleic acid (mRNA) and protein delivery to the intracellular space provide a temporary presence of the protein inside the cell, leading to no long-term concerns since the protein will eventually be turnover, and in the case of mRNA, the delivered sequence will be degraded over time preventing further expression of the protein. In this project the protein delivery method was chosen.

In order to do so it was tested if a catalytically active recombinant AOX could be produced in heterologous systems and delivered to the respiratory chain of mammalian cells.

#### 4.1.1- Plasmid engineering

In order to increase the yield of recombinant protein extracted, used engineered plasmids contained a SUMO protein sequence upstream of the AOX sequence, to prevent incorporation of the AOX protein in the bacterial mitochondrial membranes and increase its solubility in the cytosol. Furthermore, to improve the efficiency of transfection of the purified protein, an 11 amino acid TAT sequence was added in one of the set of plasmids. TAT conjugation should provide a direct import of the protein to the intracellular space<sup>(45)</sup> negating the need for a specific transfection treatment to the cells. TAT protein conjugation system was used to deliver Ndi1 to the mitochondria of mice heart cells<sup>(49, 50)</sup>, proving that its import does not compromise the mitochondrial import sequence. Also, *in silico* analysis of recombinant TAT-AOX sequence showed that TAT does not affect AOX's mitochondrial import sequence.

#### **4.1.2- Protein production**

Due to AOX being a mitochondrial membrane protein, it was expected that some of the amount of produced protein would be integrated into the membranes, despite the presence of the SUMO protein, the result of the protein production was challenging since most of the protein was being incorporated into the membrane. By decreasing the growth temperature, thus slowing down the growth rate as well as protein incorporation into the membrane, an increase of the amount of protein in the soluble fraction was achieved, this increase was higher when using the *E. coli* Rosetta 2 strain. Reasons behind the different results in *E.coli* strains are unknown, although it can be proposed that it was due to differences in some metabolic pathways taking in account that Roseta 2 are a derivate of BL21, designed to enhance the expression of eukaryotic proteins <sup>(55)</sup>.

When supplementing the medium with iron salts, due to the presence of a di-iron centre in one of the AOX subunits structure, an increase in the amount of protein in the membranes was observed. Knowing that the presence of the di-iron centre is crucial for the protein catalytic activity, it can be assumed that with a slower growth rate (30 °C), the iron integration, in native bacterial culture conditions, into the recombinant protein produced is lower. Therefore, the observed increased in the amount of the protein in its soluble form, might the soluble protein produced was not catalytically active. However, this latest fact did not give rise to any concern since the protein could receive the iron needed to be active inside the transfected cells, and if proven to be insufficient to be catalytically active, an iron supplementation of the protein could be facilitated by transferring the soluble protein to an iron enriched buffer.

#### **4.1.3- Protein purification**

Purification of recombinant AOX from the bacterial protein extract was successful on the first try, the inability to obtain a highly pure protein was expected by taking into consideration that a crude extract was used, further purifications with increased affinity for the HIS tag would be needed to produce a highly pure protein.

Imidazole presence in the cleavage buffer proved to be a crucial addition to keeping the TAT-AOX protein soluble upon the removal of the SUMO protein, in the absence of imidazole in the buffer the samples corresponding to the cleavage protein showed no band both in the Western blot and in the SDS-page for the TAT- AOX, thus suggesting a loss of protein by precipitation.

However despite the success in removing the SUMO protein and keeping the protein soluble, further purification of the protein in order to separate it from the cleaved SUMO protein and remaining bacterial proteins, proved unseccessful. Band

corresponding to TAT-AOX disappeared after being passed through the column suggesting that the protein was being trapped inside the column without the possibility of extracting it. Knowing that it is possible to purify trypanosomal AOX<sup>(62)</sup>, and having access to a 3D structural model of the *Ciona intestinalis* AOX using *Trypanosome* AOX as a template for homology modelling (Figure 3), it is possible to extrapolate that the two extra highly charged loops in the *Ciona intestinalis* AOX might interact with the column matrix therefore trapping the protein inside the column. One solution to this problem may be to change or remove the matrix inside the column preventing the trapping of the TAT-AOX.

Using alternative production and purification methods such as an *E. coli* based cell free protein synthesis system with liposome supplementation might be a solution to producing a highly pure recombinant AOX. So far, this system has been successful for production of membrane proteins (category in which AOX is included) in soluble form without toxicity or inhibitory condition to the host. Integration into extracellular liposomes, allows a protein purification by targeting the liposomes<sup>(63)</sup>, enhance providing a highly pure protein without unidentified bacterial proteins.

#### **4.1.4- TAT AOX activity assay**

In the *in vitro* assay by comparing the confluence reached between the controls, it was possible to observe that number of viable cells in the culture exposed to the TAT-AOX was significantly less than the ones present in both the WT and AOX controls. Furthermore, concentrations of TAT-AOX higher than 0.027 µg/µL lead to the death of the entire culture, in a period less than 3 h.

TAT protein deleterious role in the development and progression of HIV related neurodegenerative diseases has already been demonstrated in various studies<sup>(64, 65)</sup>, furthermore TAT toxicity in cell transfect assays has been observed with TAT concentrations of 100 µM or higher<sup>(66)</sup>. Non-disregarding TAT cytotoxic role in cellular assays, in this work it was proposed that the unidentified bacterial proteins, present in the enriched TAT-AOX extract, were to some extent toxic to the culture. Therefore by using an ultra-pure TAT-AOX solution, no toxicity effects should be observed in mammalian cells. However, in the event of the observation of a toxicity effect with an ultra-pure TAT-AOX solution an alternative protein conjugation method, such as antennapedia conjugation<sup>(66, 67)</sup>, could be employed to avoid toxic effects on cells.

The observed toxicity of the enriched TAT-AOX extract could also be the reason for the low (less than 60%) TAT-AOX success of transfection observed in the exposed cells incubated with AMA. By comparing the physiological response to AMA incubation between WT and AOX cell lines, it is safe to conclude that only cells containing AOX

were able to remain viable, by performing a bypass of the lethal blockade caused by AMA. Therefore, it can be concluded that all cells exposed to TAT-AOX which were able to remain viable after AMA incubation, had been positively transfected with a catalytically active AOX.

Western blot using protein extracts from the cells incubated with TAT-AOX was attempted, however no AOX was detected in the extract. Absence of AOX in the blot could be explained by many facts; such as the amount of protein used was considered small (less than 10 µg), the diluted amount of protein will not be completely removed from the medium by cellular uptake, by harvesting the cells there is always some protein loss due to cell undergoing apoptosis, the protein extract does not solubilize every single protein in the cells and lastly that the Western blot technique also has some protein loss associated to it in the blotting of the proteins from the SDS gel to the nitrocellulose membrane, therefore it was possible that amount of AOX protein was not enough to be detected.

Time limitations allowed for only one replicate of the experiment, however taking in consideration both visual analysis as well as the quantification of viable cells we have strong evidence that the TAT-AOX was incorporated and catalytically active. Further activity assays with an inactive TAT-AOX (such catalytically inactive AOX mutant) serving as a negative control, complemented with antibody staining of the cells might help to support this evidence showing method allows an effective delivery of a catalytically active AOX to mammalian cells.

To analyse the incorporation and catalytic activity of the enriched TAT-AOX extract in mammal tissues, it was asked the help of Natascha Sommer's laboratory to perform an *ex vivo* assay, using a perfused mouse lung. According to her readout, TAT-AOX was positively incorporated into the lung cells and was catalytically active. Furthermore, by analysing the results provided it was possible to observe that perfusion of a WT mouse lung under hypoxic challenge, with a TAT-AOX diluted physiological buffer, successfully blunted the high value in pressure gradient, thus correlating with the physiological behaviour of AOX heterozygous lung. Obtained *ex-vivo* results, suggests that the delivery system has the potential to work in an *in vivo* assay, however due to the limitations of an *ex-vivo* assay, endocrine and immunity systems responses to the presence of TAT-AOX were not evaluated.

Despite the promising result, such *ex-vivo* assays requires the use of a catalytically inactive TAT-AOX, to validate the readout that the neutralization of the hypoxia pressure was related to the incorporation of a catalytically active AOX and not to the perfusion of the lung with a protein supplemented physiological buffer.

## 4.2- AOX protection against CSE damage

From the more than 5000 hazards components in CS<sup>(11)</sup>, cyanide and carbon monoxide are known inhibitors of complex IV, furthermore it has been shown that cigarette smoke is able to cause a deadly blockade in the respiratory chain and shifting the cell death mechanism from apoptosis to necrosis<sup>(36)</sup>. This is due to a depletion of ATP inside the cell which makes the cell unable to withstand the energy required to undergo apoptosis. Taking into account previous data, it could be drawn a conclusion that if the blockade is bypassed and the ATP production maintained, by using an alternative oxidase such as AOX with the ability to bypass blockades in the cytochrome part of the respiratory chain<sup>(38)</sup>, cells may be protected against CS damage. To test this hypothesis three different AOX cell lines with their respective WT controls were used.

### 4.2.1- 293T HEK cells

In the experiments using the 293T HEK cells, a well-to-well error was associated with all the quantification performed. This was due to the cells easy detach from the plates surfaces, at room temperature, with a little pressure or harsh handling conditions. Polylysine coated plates, proved to be effective in decreasing the well-to-well error, but unable to prevent it. Therefore, for technical reasons the data collected cannot be used to reach any conclusions regarding the protective effect of AOX. Optimization of the experiments set up with the ability to quantify the detached number of cells in each step of medium replacement, would provide a way to normalize all readings thus reducing the well-to-well error associated with the quantification assay.

### 4.2.2- MEFs from Aox-Rosa26

MEFs cell lines were produced by Praveen from *AOX<sup>Rosa26</sup>* mice. Briefly, mice were generated by a site-directed integration of *Ciona intestinalis* AOX into the ROSA26<sup>(68)</sup> locus *via* homologous recombination, where a strong and ubiquitous CAG promoter controls its expression (unpublished data). AOX protein was expressed ubiquitous in all tissues (unpublished data). Despite its high expression level, AOX had no obvious adverse effect on the general mouse phenotype or expression levels of other mitochondrial respiratory chain subunits (unpublished data). AOX RNA expression was analyzed by Northern blotting which correlated with the protein expression levels. Where expressed, AOX confers respiratory resistance to azide and AMA (unpublished data).

Initially, cells were grown in medium containing 20% FBS, thus it was decided to use the same growth condition for the assays with a long term CSE incubation (48 h). CSE concentrations in which cells were able to remain viable, were shown to be much lower in the MEFs than in the 293T HEK, although the reason for such was not scrutinised as the two cell lines were physiologically different and thus different intracellular conditions and metabolism were most likely the cause.

Due to the absence of a significant difference in physiological response between the AOX cells and their respective WT to CSE incubation, it was hypothesized that the cause could be the protective effect that FBS plays in the growth medium<sup>(69)</sup>. With the thought that it was neutralizing or blocking the effect of the compounds that caused a deadly blockade by interacting with the respiratory chain, therefore preventing AOX to confer any protection since the damage was not being caused at the respiratory chain level. Validation of this hypothesis with AMA incubation, resulted in a decrease of the FBS concentration in the medium to 5%. Both 24 h and 48 h CSE incubation showed to have no difference in physiological response between AOX cells and their respective WT control, thus indicating that the presence of AOX was not able to protect the cells against CSE damage.

Successive lack of a protective AOX effect in experiments performed with both 293T HEK and MEFs cell lines, led reconsidering the experimental design. A synchronize the cells in G0 phase, an incubation step with a restrictive serum concentration for 24 h was performed followed by a 48 h long term CSE incubation. In these set of experiments only galactose medium was tested, as AOX copes with a high reduction of the respiratory chain. By using growth conditions that favour OXPHOS respiration the possible difference in physiological response between cell lines, would be increased. The obtained results showed that the presence of AOX does not provide any protection against CSE damage, enabling to exclude the hypothesis that the protective AOX effect could have been masked by the desynchronized growth of the cultures.

Taking into account that there were unpublished preliminary results obtained by Manish Kumar, a collaborator researcher in a laboratory in Bad Nauheim, showing that the presence of AOX conferred some protection against CSE damaged in NIH 3T3 cell lines, it was decided to repeat the experimental approach used for MEFs in NIH 3T3 cells to corroborate the obtained MEFs results or to show that for some unknown reason the cells were not behaving as fibroblast cells.

#### **4.2.3- NIH 3T3 cells**

Due to some technical problems, NIH 3T3 AOX cell lines needed to be produced anew, thus the number of replicates of each experiment was not higher than two. Results obtained for a 24 h CSE incubation, both low glucose and galactose medium showed no significant difference in physiological response between the AOX cells and their respective WT controls. Same result was observed for the 48 h CSE incubation in galactose medium, with and without a culture growth synchronization by serum restriction. Lethal CSE concentration for the NIH 3T3 cell was similar to one for MEFs. Obtained with the NIH 3T3 cells corroborate those obtained with the previous tested cell lines, leading to three possible conclusions.

First, was that based solely on the results obtained in this work, the problem lay not in the experiment but in the concept that it tries to prove showing that AOX might be unable to prevent any damage caused by CSE, therefore not having any protective effect on the cells against CS damage.

Second, was that the produced CSE might not be the same standard CSE used when producing the preliminary results, resulting in a loss, either by neutralization or volatilization, of some key components that interact with the respiratory chain such as cyanide which is highly unstable under cell culture conditions<sup>(70)</sup>. Therefore maintaining the CSE deadly effect due to the other thousands of compounds solubilized in the medium, but preventing AOX protection due to the inexistence of a blockade in the cytochrome chain.

The last possible conclusion was that although there were some preliminary data that AOX protects the cells from CSE damage, at this point, for some unclear reason, the cells behaved differently in both works. Thus making it unable to determine if AOX might have potential applications for protecting cells against CS damage, without further studies in the subject.

In order to be able to determine which is the correct conclusion the most efficient option would be to ask to a collaborating laboratory, experienced in CSE assays, to replicate the results obtained in this work. In doing so it, would provide a comparison of the produced CSE as a validation of either the results obtained in this work or the preliminary results of AOX protective effect in NIH 3T3 cells. Further steps can also be taken by testing not only cell viability but also other physiological processes such as apoptosis versus necrosis ratio, proliferation and autophagy.

However, considering the limitations of using CSE, which mostly contains the aqueous soluble components of CS, testing CSE exposure alone is not enough. Further studies using alternatives toxins extraction methods, such as cigarette smoke condensate (CSC) production by collecting the particulated phase the CS in a filter and

diluting in dimethyl sulfoxide (DMSO)<sup>(71)</sup>, or even direct smoke exposure using 'whole smoke exposure systems'<sup>(72)</sup>, should be performed before reaching any conclusions regarding potential AOX clinical applications in CS health issues.

### 4.3- Conclusion

The use of alternative enzymes to attenuate mitochondrial disease phenotypes is a growing field with many possible applications. In this work it was attempted to purify a recombinant AOX that could be delivered to the respiratory chain of mammalian cells while retaining its catalytic activity, as well as to analyse the use of AOX as a protective treatment against CS damage.

Production and purification of a recombinant AOX was achieved. Further optimization of the process will provide a highly pure recombinant protein. Strong evidence, both *in vitro* and *ex vivo*, regarding recombinant protein catalytic activity and ability to transfect cells were presented in this work. Upon validation, clinical applications using the recombinant AOX can be tested in *in vivo* systems.

Results obtained in this work suggest that AOX does not confer protection against CSE damage. Further studies in the subject are needed to conclude about AOX clinical applications in CS health issues.

Summarising this work provided a protocol to produce a catalytically active AOX in heterologous systems and scientific data about the use of AOX to confer protection against CS.

## References

1. Millar AH, Whelan J, Soole KL, Day DA. Organization and regulation of mitochondrial respiration in plants. *Annu Rev Plant Biol.* 2011;62:79-104.
2. Rustin P, Jacobs HT. Respiratory chain alternative enzymes as tools to better understand and counteract respiratory chain deficiencies in human cells and animals. *Physiol Plant.* 2009;137(4):362-70.
3. Dassa EP, Dufour E, Goncalves S, Jacobs HT, Rustin P. The alternative oxidase, a tool for compensating cytochrome c oxidase deficiency in human cells. *Physiol Plant.* 2009;137(4):427-34.
4. Dassa EP, Dufour E, Goncalves S, Paupe V, Hakkaart GA, Jacobs HT, et al. Expression of the alternative oxidase complements cytochrome c oxidase deficiency in human cells. *EMBO Mol Med.* 2009;1(1):30-6.
5. El-Khoury R, Dufour E, Rak M, Ramanantsoa N, Grandchamp N, Csaba Z, et al. Alternative oxidase expression in the mouse enables bypassing cytochrome c oxidase blockade and limits mitochondrial ROS overproduction. *PLoS Genet.* 2013;9(1):e1003182.
6. Fernandez-Ayala DJ, Sanz A, Vartiainen S, Kemppainen KK, Babusiak M, Mustalahti E, et al. Expression of the *Ciona intestinalis* alternative oxidase (AOX) in *Drosophila* complements defects in mitochondrial oxidative phosphorylation. *Cell Metab.* 2009;9(5):449-60.
7. Hakkaart GA, Dassa EP, Jacobs HT, Rustin P. Allotopic expression of a mitochondrial alternative oxidase confers cyanide resistance to human cell respiration. *EMBO Rep.* 2006;7(3):341-5.
8. WHO. Report on the Global Tobacco Epidemic: Enforcing bans on tobacco advertising, promotion and sponsorship. Geneva: World Health Organization., 2013.
9. van der Vaart H, Postma DS, Timens W, ten Hacken NH. Acute effects of cigarette smoke on inflammation and oxidative stress: a review. *Thorax.* 2004;59(8):713-21.
10. Yanbaeva DG, Dentener MA, Creutzberg EC, Wesseling G, Wouters EF. Systemic effects of smoking. *Chest.* 2007;131(5):1557-66.
11. Talhout R, Schulz T, Florek E, van Benthem J, Wester P, Opperhuizen A. Hazardous compounds in tobacco smoke. *Int J Environ Res Public Health.* 2011;8(2):613-28.
12. Agarwal AR, Yin F, Cadenas E. Short-term cigarette smoke exposure leads to metabolic alterations in lung alveolar cells. *Am J Respir Cell Mol Biol.* 2014;51(2):284-93.
13. Aravamudan B, Kiel A, Freeman M, Delmotte P, Thompson M, Vassallo R, et al. Cigarette smoke-induced mitochondrial fragmentation and dysfunction in human airway smooth muscle. *Am J Physiol Lung Cell Mol Physiol.* 2014;306(9):L840-54.
14. Murphy MP. How mitochondria produce reactive oxygen species. *Biochem J.* 2009;417(1):1-13.
15. Leavesley HB, Li L, Prabhakaran K, Borowitz JL, Isom GE. Interaction of cyanide and nitric oxide with cytochrome c oxidase: implications for acute cyanide toxicity. *Toxicol Sci.* 2008;101(1):101-11.
16. Alonso JR, Cardellach F, Lopez S, Casademont J, Miro O. Carbon monoxide specifically inhibits cytochrome c oxidase of human mitochondrial respiratory chain. *Pharmacol Toxicol.* 2003;93(3):142-6.
17. Henry BA, Andrews ZB, Rao A, Clarke IJ. Central Leptin Activates Mitochondrial Function and Increases Heat Production in Skeletal Muscle. *Endocrinology.* 2011;152(7):2609-18.
18. Glancy B, Balaban RS. Role of mitochondrial Ca<sup>2+</sup> in the regulation of cellular energetics. *Biochemistry.* 2012;51(14):2959-73.
19. Tait SW, Green DR. Mitochondria and cell signalling. *J Cell Sci.* 2012;125(Pt 4):807-15.
20. Borutaite V. Mitochondria as decision-makers in cell death. *Environ Mol Mutagen.* 2010;51(5):406-16.

21. Labbe K, Murley A, Nunnari J. Determinants and functions of mitochondrial behavior. *Annu Rev Cell Dev Biol.* 2014;30:357-91.
22. Green DR, Galluzzi L, Kroemer G. Mitochondria and the autophagy-inflammation-cell death axis in organismal aging. *Science.* 2011;333(6046):1109-12.
23. Alberts B, Johnson A, Lewis J, Raff M, Roberts K, Walter P. Cell Chemistry and Biosynthesis. *Molecular Biology of the Cell.* 5th ed: Garland Science; 2008. p. 45-124.
24. Alberts B, Johnson A, Lewis J, Raff M, Roberts K, Walter P. Energy conversion: Mitochondria and Chloroplast. *Molecular Biology of the Cell.* 5th ed: Garland Science; 2008. p. 813-78.
25. Aguer C, Gambarotta D, Mailloux RJ, Moffat C, Dent R, McPherson R, et al. Galactose Enhances Oxidative Metabolism and Reveals Mitochondrial Dysfunction in Human Primary Muscle Cells. *PLoS ONE.* 2011;6(12):e28536.
26. Le A, Lane AN, Hamaker M, Bose S, Gouw A, Barbi J, et al. Glucose-independent glutamine metabolism via TCA cycling for proliferation and survival in B cells. *Cell Metab.* 2012;15(1):110-21.
27. Fan J, Kamphorst JJ, Mathew R, Chung MK, White E, Shlomi T, et al. Glutamine-driven oxidative phosphorylation is a major ATP source in transformed mammalian cells in both normoxia and hypoxia. *Mol Syst Biol.* 2013;9:712.
28. Berg JM, Tymoczko JL, Stryer L, Gregory J. Gatto J. Oxidative phosphorylation. *Biochemistry.* 7th ed. New York: W. H. Freeman and Company; 2012. p. 525-64.
29. Trumpower BL. The protonmotive Q cycle. Energy transduction by coupling of proton translocation to electron transfer by the cytochrome bc1 complex. *J Biol Chem.* 1990;265(20):11409-12.
30. Das AM. Regulation of the mitochondrial ATP-synthase in health and disease. *Mol Genet Metab.* 2003;79(2):71-82.
31. Sena LA, Chandel NS. Physiological roles of mitochondrial reactive oxygen species. *Mol Cell.* 2012;48(2):158-67.
32. Brand MD. The sites and topology of mitochondrial superoxide production. *Exp Gerontol.* 2010;45(7-8):466-72.
33. Lambert AJ, Brand MD. Reactive oxygen species production by mitochondria. *Methods in molecular biology (Clifton, NJ).* 2009;554:165-81.
34. WHO. Global report: Mortality attributed to Tobacco. Geneva: World Health Organization., 2012.
35. Li X, Zhang Y, Yeung SC, Liang Y, Liang X, Ding Y, et al. Mitochondrial transfer of induced pluripotent stem cell-derived mesenchymal stem cells to airway epithelial cells attenuates cigarette smoke-induced damage. *Am J Respir Cell Mol Biol.* 2014;51(3):455-65.
36. van der Toorn M, Slebos DJ, de Bruin HG, Leuvenink HG, Bakker SJ, Gans RO, et al. Cigarette smoke-induced blockade of the mitochondrial respiratory chain switches lung epithelial cell apoptosis into necrosis. *Am J Physiol Lung Cell Mol Physiol.* 2007;292(5):L1211-8.
37. McDonald A, Vanlerberghe G. Branched mitochondrial electron transport in the Animalia: presence of alternative oxidase in several animal phyla. *IUBMB Life.* 2004;56(6):333-41.
38. Affourtit C, Albury MS, Crichton PG, Moore AL. Exploring the molecular nature of alternative oxidase regulation and catalysis. *FEBS Lett.* 2002;510(3):121-6.
39. El-Khoury R, Kempainen KK, Dufour E, Szibor M, Jacobs HT, Rustin P. Engineering the alternative oxidase gene to better understand and counteract mitochondrial defects: state of the art and perspectives. *Br J Pharmacol.* 2014;171(8):2243-9.
40. Rustin P, Queiroz-Claret C. Changes in oxidative properties of *Kalanchoe blossfeldiana* leaf mitochondria during development of Crassulacean acid metabolism. *Planta.* 1985;164(3):415-22.
41. Bahr JT, Bonner WD, Jr. Cyanide-insensitive respiration. I. The steady states of skunk cabbage spadix and bean hypocotyl mitochondria. *J Biol Chem.* 1973;248(10):3441-5.

42. Bahr JT, Bonner WD, Jr. Cyanide-insensitive respiration. II. Control of the alternate pathway. *J Biol Chem.* 1973;248(10):3446-50.
43. Green M, Loewenstein PM. Autonomous functional domains of chemically synthesized human immunodeficiency virus tat trans-activator protein. *Cell.* 1988;55(6):1179-88.
44. Frankel AD, Pabo CO. Cellular uptake of the tat protein from human immunodeficiency virus. *Cell.* 1988;55(6):1189-93.
45. Wadia JS, Dowdy SF. Protein transduction technology. *Curr Opin Biotechnol.* 2002;13(1):52-6.
46. Schwarze SR, Hruska KA, Dowdy SF. Protein transduction: unrestricted delivery into all cells? *Trends Cell Biol.* 2000;10(7):290-5.
47. Watson K, Edwards RJ. HIV-1-trans-activating (Tat) protein: both a target and a tool in therapeutic approaches. *Biochemical pharmacology.* 1999;58(10):1521-8.
48. de Vries S, Grivell LA. Purification and characterization of a rotenone-insensitive NADH:Q6 oxidoreductase from mitochondria of *Saccharomyces cerevisiae*. *Eur J Biochem.* 1988;176(2):377-84.
49. Perry CN, Huang C, Liu W, Magee N, Carreira RS, Gottlieb RA. Xenotransplantation of mitochondrial electron transfer enzyme, Ndi1, in myocardial reperfusion injury. *PLoS One.* 2011;6(2):e16288.
50. Mentzer RM, Jr., Wider J, Perry CN, Gottlieb RA. Reduction of infarct size by the therapeutic protein TAT-Ndi1 in vivo. *J Cardiovasc Pharmacol Ther.* 2014;19(3):315-20.
51. Johnson ES. Protein modification by SUMO. Annual review of biochemistry. 2004;73:355-82.
52. Terpe K. Overview of bacterial expression systems for heterologous protein production: from molecular and biochemical fundamentals to commercial systems. *Applied microbiology and biotechnology.* 2006;72(2):211-22.
53. Eva R, Bram DC, Joery DK, Tamara V, Geert B, Vera R, et al. Strategies for immortalization of primary hepatocytes. *Journal of Hepatology.* 2014;61(4):925-43.
54. Roemer E, Schramke H, Weiler H, Buettner A, Kausche S, Weber S, et al. Mainstream Smoke Chemistry and In Vitro and In Vivo Toxicity of the Reference Cigarettes 3R4F and 2R4F. *Contributions to Tobacco Research.* 2012;25(1).
55. Rosano GL, Ceccarelli EA. Recombinant protein expression in *Escherichia coli*: advances and challenges. *Frontiers in Microbiology.* 2014;5:172.
56. Mahmoudi S, Abtahi H, Bahador A, Mosayebi G, Salmanian AH, Teymuri M. Optimizing of Nutrients for High Level Expression of Recombinant Streptokinase Using pET32a Expression System. *Maedica (Buchar).* 2012;7(3):241-6.
57. Seddon AM, Curnow P, Booth PJ. Membrane proteins, lipids and detergents: not just a soap opera. *Biochimica et Biophysica Acta (BBA) - Biomembranes.* 2004;1666(1-2):105-17.
58. Karla W, Shams H, Orr JA, Scheid P. Effects of the thromboxane A2 mimetic, U46,619, on pulmonary vagal afferents in the cat. *Respir Physiol.* 1992;87(3):383-96.
59. Liu F, Carrithers JA, Shirer HW, Orr JA. Thromboxane A2 mimetic, U46,619, and slowly adapting stretch receptor activity in the rabbit. *Respir Physiol.* 1992;88(1-2):77-86.
60. Sommer N, Dietrich A, Schermuly RT, Ghofrani HA, Gudermann T, Schulz R, et al. Regulation of hypoxic pulmonary vasoconstriction: basic mechanisms. *The European respiratory journal.* 2008;32(6):1639-51.
61. Langan TJ, Chou RC. Synchronization of mammalian cell cultures by serum deprivation. *Methods in molecular biology (Clifton, NJ).* 2011;761:75-83.
62. Kido Y, Sakamoto K, Nakamura K, Harada M, Suzuki T, Yabu Y, et al. Purification and kinetic characterization of recombinant alternative oxidase from *Trypanosoma brucei brucei*. *Biochimica et Biophysica Acta (BBA) - Bioenergetics.* 2010;1797(4):443-50.
63. Nozawa A, Ogasawara T, Matsunaga S, Iwasaki T, Sawasaki T, Endo Y. Production and partial purification of membrane proteins using a liposome-supplemented wheat cell-free translation system. *BMC biotechnology.* 2011;11:35.

64. Bagashev A, Sawaya BE. Roles and functions of HIV-1 Tat protein in the CNS: an overview. *Virology journal*. 2013;10:358.
65. Gendelman HE, Grant I, Everall IP, Fox HS, Gelbard HA, Lipton SA, et al. Immunodeficient mice. *The Neurology of AIDS*. 3rd ed: Oxford University Press; 2012.
66. Jones SW, Christison R, Bundell K, Voyce CJ, Brockbank SMV, Newham P, et al. Characterisation of cell-penetrating peptide-mediated peptide delivery. *British Journal of Pharmacology*. 2005;145(8):1093-102.
67. Garcia-Echeverria C, Jiang L, Ramsey TM, Sharma SK, Chen YP. A new Antennapedia-derived vector for intracellular delivery of exogenous compounds. *Bioorganic & medicinal chemistry letters*. 2001;11(11):1363-6.
68. Perez-Pinera P, Ousterout DG, Brown MT, Gersbach CA. Gene targeting to the ROSA26 locus directed by engineered zinc finger nucleases. *Nucleic Acids Research*. 2012;40(8):3741-52.
69. Francis GL. Albumin and mammalian cell culture: implications for biotechnology applications. *Cytotechnology*. 2010;62(1):1-16.
70. Arun P, Moffett JR, Ives JA, Todorov TI, Centeno JA, Namboodiri MA, et al. Rapid sodium cyanide depletion in cell culture media: outgassing of hydrogen cyanide at physiological pH. *Anal Biochem*. 2005;339(2):282-9.
71. Narayan S, Jaiswal AS, Kang D, Srivastava P, Das GM, Gairola CG. Cigarette smoke condensate-induced transformation of normal human breast epithelial cells in vitro. *Oncogene*. 2004;23(35):5880-9.
72. Thorne D, Adamson J. A review of in vitro cigarette smoke exposure systems. *Experimental and Toxicologic Pathology*. 2013;65(7-8):1183-93.